Coordination Chemistry Reviews 253 (2009) 1221–1247

Contents lists available at ScienceDirect

Coordination Chemistry Reviews

journal homepage: www.elsevier.com/locate/ccr

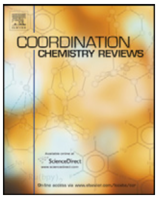

Review

Solvothermal synthesis of Group 13–15 chalcogenidometalates with chelating organic amines

Jian Zhou[a], Jie Dai[a,b,*], Guo-Qing Bian[a], Chun-Ying Li[a]

[a] *Department of Chemistry and Key Laboratory of Organic Synthesis of Jiangsu Province, Suzhou University, Suzhou 215123, PR China*
[b] *State Key Laboratory of Coordination Chemistry, Nanjing University, Nanjing 210093, PR China*

Contents

1. Introduction 1222
2. Roles of the chelating amines in solvothermal syntheses of chalcogenidometalates 1222
   2.1. Chelating amines used as medium for solvothermal reaction 1222
   2.2. Template or structure directing effects of the chelating amines 1223
   2.3. Structures and structural influences of the saturated complex cations 1223
   2.4. Properties and structural influences of the unsaturated complex cations 1228
3. Structures of Group 13–15 chalcogenidometalates 1231
   3.1. Chalcogenidometalates with discrete metal complex cations 1231
      3.1.1. Crystal structures of Group 13 chalcogenidometalate (Ga, In) anions 1232
      3.1.2. Crystal structures of Group 14 chalcogenidometalate (Ge, Sn) anions 1234
      3.1.3. Crystal structures of Group 15 chalcogenidometalate (As, Sb) anions 1235
   3.2. Chalcogenidometalates with covalently linked metal complex cations 1237
      3.2.1. Crystal structures of Group 13 chalcogenidometalates (Ga, In) 1237
      3.2.2. Crystal structures of Group 14 chalcogenidometalates (Ge, Sn) 1238
      3.2.3. Crystal structures of Group 15 chalcogenidometalates (As, Sb) 1243
4. Summary 1246
   Acknowledgements 1246
   References 1246

ARTICLE INFO

Article history:
Received 16 February 2008
Accepted 22 August 2008
Available online 3 September 2008

Keywords:
Chalcogenidometalates
Solvothermal synthesis
Chelate amines
Metal complex

ABSTRACT

Inorganic–organic hybrid chalcogenidometalate materials have attracted considerable interest, because they are a new type of materials with unique topologic structures. The syntheses of these materials are typically carried out under hydro(solvo)thermal conditions at relatively low temperatures. Organic amines have been demonstrated to be successful and versatile molecules to be used in template-directed synthesis of numerous chalcogenide-based open-framework materials. Some comprehensive reviews have summarized the preparation and structures of the chalcogenidometalates with non-chelating amines. Extended and embedded researches on the chelating amines containing a different number of *N*-donor atoms have recently attracted more interest in synthetic chemistry. A series of unique inorganic–organic hybrid chalcogenidometalate materials are successfully isolated lately. This review focuses on the recent developments in solvothermal synthesis of main group chalcogenidometalates in the presence of organic chelating amines or polyamines as reaction medium. In contrast to the non-chelating amines, the roles of the chelating amines in the syntheses and the effects of the chelating amines on the crystal structures are discussed. A comprehensive outline of the chalcogenidometalate compounds with metal complex cations is also presented.

Abbreviations: atep, 4-(2-aminoethyl)triethylenetetramine; chxn, *trans*-1,2-diaminocyclohexane; cyclam, tetramine 1,4,8,11-tetraazacyclotetradecane; dap, diaminopropane; dape, 1,3-diaminopentane; dien, diethylenetriamine; en, ethylenediamine; mdap, *N*-metyl-1,3-diaminopropane; tepa, tetraethylenepentamine; teta, triethylenetetramine; tren, tris(2-aminoethyl)amine.

E-mail address: daijie@suda.edu.cn (J. Dai).

0010-8545/$ – see front matter © 2008 Elsevier B.V. All rights reserved.
doi:10.1016/j.ccr.2008.08.015

1. Introduction

Inorganic–organic hybrid chalcogenidometalate materials of the heavier Group 13–15 elements have attracted considerable interest, because they are a new type of materials with unique topologic structures integrating properties of classical electronics, optics and semiconductor materials [1]. The syntheses of these materials are typically carried out under hydro(solvo)thermal conditions in polarizing solvents such as water, the alcohol and organic amines at relatively low temperatures ($T \approx 100–200\,^{\circ}\mathrm{C}$) [2]. A classical review article on thio- and selenidometalates of Group 13–14 elements with alkali and alkaline-earth metal cations, which were prepared in water, has appeared in 1983 [3]. Then solvothermal reactions by employing alcohol as solvent have afforded an extensive range of new alkali metal chalcogenides [4]. A comprehensive review of the application of mild solvothermal techniques to the preparation of chalcogenidometalates of Group 14–15 elements with alkali, alkaline earth, or organic cations (such as R_4N^+, Ph_4P^+) has been given by Sheldrick and Wachhold [2a] in 1997. The crystal structures of these type compounds, in as comprehensive and systematic manner as possible, have been discussed later in another review article, the same group in 1998 [5].

Since the early work by Bedard et al. in 1989, who prepared thio- and selenidometalates by using alkylammonium cations R_4N^+ (R = Me, Et, Pr, etc.) as template agents under hydrothermal conditions [1f], the synthetic approaches were developed applying amines for the preparation of chalcogenidometalates of Group 13–15 elements [6]. Subsequent developments in template-directed synthesis of these materials have resulted in numerous chalcogenide-based open-framework materials [1,6]. Recently, Yaghi, Parise, Feng and their co-workers have investigated Group 13 and 14 thio- and selenidometalates by using unique non-chelating amines as template agents. They have obtained a number of zeolite analogs constructed by supertetrahedral clusters under relatively mild conditions [1a,c,6c,7]. The structural architectures of zeotype Group 13/14 chalcogenidometalates, with protonated non-chelating amines as counterions, has been summarized in an important review article by Feng et al. in 2005 [8]. In 1996, Stephan and Kanatzidis reported a 2D cobalt thioantimonate $[Co(en)_3]CoSb_4S_8$ using an aqueous solution of a chelating amine (ethylenediamine) [9]. A large number of new Group 15 thio- and selenidometalates with transition metal amino complexes were later isolated by Bensch and co-workers under the solvothermal conditions [10]. Li et al. have exploited some selenide and telluride systems of the main Group 13–15 elements in solvothermal synthesis using en as a reaction medium in the same period of time and a review article of corresponding chalcogenidometalates has been published in 1999 [2c]. A very new article reviewed the ternary M/14/16 chalcogenidometalates and some of the compounds contain metal coordinated amines [2d]. However, only ethylenediamine and limited transition metal complexes are involved in these reviews.

Extended and embedded researches on the chelating amine ligands containing a different number of *N*-donor atoms for preparation of inorganic–organic hybrid chalcogenidometalate materials are appeared in the following years [11]. Bensch and co-workers prepared transition metal thiostannates with various polyamine ligands in order to investigate the influence of the amine ligands onto the structure of these compounds [11b]. Vaqueiro synthesized transition metal thiogallates by solvothermal reaction in ethylenediamine and reported some unique polymeric structures with covalently bonded metal complex joint [11a]. Feng and co-workers reported a negatively charged Mn–Te–Sn helical chain, which is decorated with metal complexes surrounding the helices [12]. Our recent research interest has been focused on solvothermal preparation of Group 13–15 chalcogenidometalates in the presence of transition/lanthanide metal ions and chelating polyamines under solvothermal conditions. Some low dimensional new chalcogenidometalate with transition metal complexes were obtained [13] and a series of lanthanide-containing chalcogenido gallate/indates, stannates and antimonates were also successfully isolated [14].

The chelating amine is not only an excellent solvent for solvothermal synthesis of chalcogenidometalates, but at least performs two other important roles: (1) offering a chalcogenide source by reacting with chalcogen elements (redox reaction), (2) chelating transition metal or lanthanide metal ions forming large $[M(amine)_x]^{n+}$ counterions to stabilize frameworks of the chalcogen-containing anions (coordinate reaction). It is noteworthy that often metals are supplied as starting materials that are oxidized in the in situ formation of transition metal complexes. The reaction mechanism is unclear, but it is undoubted that the chelating reaction accelerates the oxidization of the metals. The proposed main reactions in the in situ formation of chalcogenidometalates are summarized as the Eqs. (1)–(3). In addition, the large metal complexes as new counterions or structure-directing agents may transfer the electronic, optical, and magnetic properties of metal complexes into the host inorganic framework or the ionic compounds, which also provide complementary properties and synergistic effects.

A disproportionation process:

$$\mathrm{Q} + \text{amine} \rightarrow \mathrm{Q}^{2-}\ (\text{or } \mathrm{Q}_m{}^{2-}) + (\text{Hamine})^{+} + \text{oxidized byproduct} \qquad (1)$$

A coordination process:

$$\mathrm{M}^{n+} + \text{amine} \rightarrow [\mathrm{M}(\text{amine})_x]^{n+} \qquad (2)$$

A redox and coordination process:

$$\mathrm{Q} + \mathrm{M} + \text{amine} \rightarrow [\mathrm{M}(\text{amine})_x]^{n+} + \mathrm{Q}^{2-}\ (\text{or } \mathrm{M}_y\mathrm{Q}_z{}^{m-}) \qquad (3)$$

As comprehensive information, typical reaction conditions that have been employed for the preparation of Group 13–15 chalcogenidometalates with in situ generated metal complexes and the reaction products have been summarized in Tables 1–3. This review will focus primarily on the hydro(solvo)thermal syntheses of 13–15 group chalcogenometalates with chelating amines and their metal complexes, which were published in recent years. The roles of the chelating amines in the syntheses and the effects of the chelating amines on the crystal structures are discussed in detail.

2. Roles of the chelating amines in solvothermal syntheses of chalcogenidometalates

2.1. Chelating amines used as medium for solvothermal reaction

Solvothermal syntheses in amines, involving the relatively low pressure (<30 bar), can generally be performed in thick-walled glass tubes and general autoclaves at relatively low temperature ($T \approx 100–200\,^{\circ}\mathrm{C}$). The potential of this technique for the preparation of solid-state chalcogenidometalates was discussed in 1997 in the article by Sheldrick and Wachhold [2a]. As a solvent the properties of the amines are very important for solvothermal synthesis of chalcogenidometalates. Physical constants for some chelating organic amines are listed in Table 4. Ethylenediamine (en) is an excellent reaction medium with appropriate boiling point and low viscosity. The polyamines, such as triethylenetetramine (teta) and tetraethylenepentamine (tepa) are well known chelating amines,

Table 1
Preparative information for the chalcogenometalates of Group 13 elements with amine complexes

	Compounds[a]	Reactants	Solvent	*d*	Space group	Reference
Anion with discrete complex cation	$[M(en)_3]_{0.5}[GaS_2]$ (M = Mn(1), Co(2), Ni(3))	$Ga_2S_3 + MCl_2 + S$ or $Ga + NiS + S$	en	1	*Cmcm*	[11a]
	$[Dy_2(en)_6(\mu_2\text{-}OH)_2]Ga_4S_8$(4)	$DyCl_3 + Ga_2S_3 + S$	en	1	$P\bar{1}$	[14g]
	$[Co(en)_3]Ga_2Se_4$(5)	Ga + Co + Se	en + H_2O	1	*Cmcm*	[13n]
	$[Mn(dap)_3]_{0.5}[GaSe_2]$(6)	Ga + Mn + Se	dap + H_2O	1	*Cmcm*	[13c]
	$[Ni(dien)_2]_{0.5}[InS_2]$(7)	$In_2S_3 + Ni + S$	dien + H_2O	1	$C2/c$	[13a]
	$[Ni(dap)_3]_{0.5}[InS_2]$(8)	$In_2S_3 + Ni + S$	dap + H_2O	1	*Cmcm*	[13a]
	$[Zn(tren)(\mu\text{-}teta)_{0.5}][InTe_2]Cl$(9)	$InCl_3 + ZnCl_2 + Te$	tren	1	$C2/c$	[13b]
	$[M(en)_3][In_2Te_4]\cdot en$ (M = Ni(10), Co(11))	$InCl_3 + MCl_2 + Te$	en	1	$P2_1/c$	[13b]
	$[M(en)_3]_2(en)_{0.5}[In_4Te_8]$ (M = Mn(12), Fe(13), Zn(14))	$InCl_3 + MCl_2$ (or Fe) + Te	en	1	$P\bar{1}$	[13b]
	$[La(en)_4Cl][In_2Te_4]$(15)	$InCl_3 + SrTe + LaCl_3 + Te$	en	1	$I4$	[15]
	$[Sm(en)_4Cl][In_2Te_4]$(16)	$InCl_3 + LaCl_3 + Te$	en	1	*Pbca*	[14h]
	$[M(en)_3][In_2Te_6]$ (M = Fe(17), Zn(18))	Li_2Te (or Cs_2Te) + $K_2Te + MCl_2 + InCl_3 + Te$	en	1	$P2_12_12_1$	[16]
	α and β-$[Mo_3(en)_3(\mu_2\text{-}Te_2)_3(\mu_3\text{-}Te)(\mu_3\text{-}O)][In_2Te_6]$(19)	$Li_2Te + K_2Te + MoCl_5 + InCl_3 + Te$	en	1	$P2_1/c(\alpha)$, $P2_1/a(\beta)$	[16]
	$[Zn(en)_3]_4\{In_{16}(Te_2)_4(Te_3)Te_{22}\}$(20)	$ZnCl_2 + InCl_3 + Te$	en	2	$C2/c$	[17]
Covalently linked cations and anions	$Mn(en)_2[Ga_2S_4]$(21)	$Ga_2S_3 + MCl_2 + S$	en	3	$C2/c$	[11a]
	$\{[Ni(tepa)]_2SO_4\}[Ni(tepa)(Ga_4S_6(SH)_4)]$(22)	Ga + NiS + S	tepa + H_2O	0	$C2/c$	[13c]
	$[Mn(atep)][Ga_2S_4]$(23)	$Ga_2S_3 + MnS + S$	tepa + H_2O	1	$P2_1/n$	[13c]
	$[Ni(tepa)]_2[In_4S_7(SH)_2]\cdot H_2O$(24)	$In_2S_3 + Ni + S$	tepa + H_2O	1	$P2_1/c$	[13a]

[a] Abbreviations for the various amine components are given at the beginning of the revirw, *d*: dimensionalities.

however, these pure amines are unsuitable for the use as medium in solvothermal synthesis in enhanced pressure for their higher boiling point and higher viscosity (Table 4). These medium being sometimes used in the reaction that only heat being needed. In this case, water is sometimes used as an auxiliary medium for solvothermal reactions. The boiling point of water (100 °C) is much lower than that of the polyamines (≈200 °C), diffusion processes for molecules and ions in a mixed solvent of water and polyamine at the intermediate temperatures (typically employed 100–200 °C) will be considerably more rapid, due to the markedly lower viscosity of water. This leads to acceleration in the solubilization of starting materials and in subsequent crystal growth (see Tables 1–3). However, the hydrophilic property for lanthanide metal ions often limits the use of water–amine medium for preparing lanthanide chalcogenidometalates due to the strong hydrolysis.

2.2. *Template or structure directing effects of the chelating amines*

Amines act as template agents or structure directing agents inducing the formation of chalcogenometalate anions and incorporate them into the final products. The protonated cations of the nonchelating organic amines as template ions have surfactant-like behavior, their hydrophilic groups point toward the anionic framework and hydrophobic groups cluster together to encircle 'voids' within the structure. An interesting example is $[(C_2H_5)_2NH_2]_7(In_{11}S_{21}H_2)$ [6f] (Fig. 1a), in which the hierarchical $[In_{10}S_{20}]^{10-}$ supertetrahedra units are interconnected by simple InS_4 tetrahedra with 3-connected mode into the $[In_{11}S_{21}H_2]^{7-}$ layers. The $[(C_2H_5)_2NH_2]^+$ cations are located in the pores of the layers. The protonated nonchelating amine groups pointing towards the thioindate ensure that the H atoms are involved in S···H interactions. The analogous $[(C_3H_7)_2NH_2]^+$ cations in $[(C_3H_7)_2NH_2]_3[In_6S_{11}H]$ [6e] are located within the framework voids of the layers constructed by InS_4 tetrahedra sharing corners and edges. While the hydrophobic organic groups (the carbon backbone) in the chelating amines or cations hided between the hydrophilic amine groups. These amine cations are usually self-arranged to a structure with strong N—H···N hydrogen bonds and act as a new type of structure director. For example, tris(2-aminoethylene)amine can take a pseudo-tetrahedron conformation, so that it is a suitable structure director for some 3D network structures with T_n building units [1a]. Another unique example is the structure of $[H_2dap]_2[Ga_4Se_8]$ [13c]. Fig. 1b shows the related positions of the chelating amine cations (blue) and the selenidogallate anions (green). The $[Ga_4Se_{10}]^{8-}$ adamantane-like building units (T_2) are linked together by their four terminal Se atoms in D_{2d} symmetry to construct a 2D network with grooves running along the surfaces of the sheet. The structure-directing agents (H_2dap cations) are arranged in a band-like structure *via* head-to-head-connected amine groups, and they are located above the grooves displaying a chessboard-like pattern. Each NH group interacts with two Se atoms from two adjacent T_2 clusters in the sheet, which implies the presence of a weak H-bonding interaction between the structure-directing agents and the anionic framework.

2.3. *Structures and structural influences of the saturated complex cations*

In most of the solvothermal reactions involving transition-metal ions, including Mn^{2+}, Fe^{2+}, Co^{2+}, Ni^{2+}, Cr^{3+}, Zn^{2+} and lanthanide metal ions (such as La^{3+}, Sm^{3+}, Nd^{3+}, Eu^{3+}), the strong chelating amines form stable metal complexes. These complex cations can be divided into saturated complex cations and unsaturated complex cations. The saturated complex cations include two types, namely mono-nuclear and dinuclear complex cations. The transition-metal ions are usually chelated by bidentate (en and dap), or tridentate (dien) chelating amines to form a distorted octahedron displaying different configurations (Fig. 2a and b). The lanthanide metal ion is chelated by bi(or tri)-dentate chelating amines to form a distorted tricapped trigonal prism (Fig. 2c) or a bicapped trigonal prism (Fig. 2d). There is no symmetry plane in $[M(en)_3]^{2+}$, as a result, such complexes can adopt either of two optical forms (Δ or Λ), however, a racemic mixture of the two forms exists usually in most of the compounds. In addition to the asymmetry generated by the coordination center, it is possible to have asymmetry in the ligand as well. For instance, the conformation of $[Zn(en)_3]^{2+}$ in $[Zn(en)_3]_2[Sn_2Te_6]$ [21] is Δ(λλδ) and in $[Zn(en)_3]_2[Sn_2S_6]$ [13f] is Δ(λλλ). Another example is the different conformation of the $[M(dien)_2]^{2+}$ octahedron. Both u-fac and mer-configurations are observed in $[Ni(dien)_2]_2[Sb_4S_8]$ [10c]. In compound $[Ni(dien)_2]_3[Sb_{12}S_{21}]\cdot H_2O$ [40a] there are two crystallographically independent $[Ni(dien)_2]^{2+}$ cations with one cation in the u-fac configuration and the second cation adopting the s-fac configuration.

The limited examples of dinuclear complex cations include $[Ln_2(en)_6(\mu_2\text{-}OH)_2]^{4+}$ (Ln = Nd, Gd) [14b,g], $[\{Mn(en)_2(enH)\}_2(\mu$-

Table 2
Preparative information for the chalcogenometalates of Group 14 elements with amine complexes

	Compounds	Reactants	Solvent	d	Space group	Reference
Anion with discrete complex cation	$[M(en)_3]_2[Sn_2S_6]$ (M = Mn(25), Co(26), Zn(27), Ni(28))	$MCl_2 + SnCl_4{\cdot}5H_2O + S$ or $Ni + Sn + S$	en	0	$C2/c$(25)[a]; $Pbca$ (26–28)	[13f,13g,11b]
	$[Ni(dien)_3]_2[Sn_2S_6]$(29)	$MCl_2 + SnCl_4{\cdot}5H_2O + S$	dien	0	$P2_1/n$	[13g]
	$[Ni(dap)_3]_2[Sn_2S_6]{\cdot}2H_2O$(30)	$Ni + Sn + S$	dap	0	$P\bar{1}$	[11b]
	$[Ln_2(en)_6(\mu_2\text{-}OH)_2][Sn_2S_6]$(Ln = Dy(31), Er(32))	$Ln_2O_3 + SnCl_4 + S$	en	0	$P2_1/n$	[14a]
	$[Ln_2(en)_6(\mu_2\text{-}OH)_2][Sn_2S_6]$ (Ln = Nd(33), Gd(34))	$LnCl_3 + SnCl_4 + S$	en	0	$P2_1/n$	[14b]
	$[Gd(dien)_3]_2[(Sn_2S_6)Cl_2]$(35)	$LnCl_3 + SnCl_4 + S$	en	0	$P2_1/n$	[14b]
	$[Mn(en)_3]_2[Sn_2S_6]{\cdot}2H_2O$(36)	$Mn + Sn + S$	en + H_2O	0	$P2_1/c$	[18]
	$[Mn(dien)_2]_2[Sn_2S_6]$(37)	$Mn + Sn + S$	dien + H_2O	0	$P2_1/c$	[18]
	$[M(en)_3]_2[Sn_2Se_6]$ (M = Ni(38), Mn(39), Zn(40))	$MCl_2 + SnSe + Se$	en	0	$Pbca$	[19,20]
	$[M(en)_3]_2[Sn_2Te_6]$ (M = Mn(41), Zn(42))	$SnTe + MnCl_2 + Te$ (or $Cs_2Te + ZnCl_2 + SnCl_2 + Te$)	en	0	$Pbca$(41) $P2_1/n$(42)	[21]
	$[Mn(en)_3]_2[Sn_2Te_6]{\cdot}4H_2O$(43)	$[Na_4(en)_4][SnTe_4] + Mn(OAc)_2{\cdot}4H_2O$	H_2O/layered by THF	0	$P\bar{1}$	[22]
	$[Mn(en)_3]_2[Sn_2Te_6]{\cdot}en$(44)	$K_4SnTe_4 + ZnCl_2 + (C_2H_5)_4NBr$	en	0	$P2_1/n$	[23]
	$[Dy_2(en)_6(\mu_2\text{-}OH)_2][Sn_2Se_6]$(45)	$Dy_2O_3 + SnCl_4 + Se$	en	0	$P2_1/n$	[14a]
	$[Mn(en)_3][CdSnTe_4]$(46)	$MnCl_2 + CdCl_2 + SnTe + Te$	en	1	$P\bar{1}$	[24]
	$[Mn(en)_3][Ag_6Sn_2Te_8]$(47)	$MnCl_2 + AgCl + SnTe + Te$	en	2	R-3m	[24]
	$[M(en)_3]_2[Ge_2S_6]$ (M = Mn(48), Ni(49))	$MCl_2{\cdot}6H_2O + GeO_2 + S$	en	0	$C2/c$(48), $Pbca$(49)	[13h]
	$[Mn(en)_3]_2[Ge_2Se_6]$(50)	$MnCl_2{\cdot}4H_2O + GeO_2 + Se$	en	0	$P2_1/n$	[13m]
	$[Fe(dien)_2]_2[Ge_2Se_6]$(51)	$FeCl_2{\cdot}4H_2O + GeO_2 + Se$	dien	0	$P2_1/n$	[13m]
	$(enH_2)[\{Mn(en)_2(enH)\}_2(\mu\text{-}en)](Ge_2Se_7)_2$(52)	$Ge + Se + Mn(Ac)_2 + [(CH_3)_2NH_2]Cl$	en + CH_3OH	0	$Pbca$	[25]
	$[Mn(dien)_2]_2[Ge_2Se_7]$(53)	$Ge + Se + Mn(Ac)_2 + NaCO_3$	en	0	$P2_1/c$	[25]
	$[Zn(tren)(H_2O)[Ge_3ZnS_9(H_2O)_2]$(54)	$GeO_2 + Zn(NO_3)_2 + S$	tren	2	$P3$	[26]
Covalently linked cations and anions	$[M(tren)]_2[Sn_2S_6]$ (M = Co(55), Ni(56))	$M + Sn + S$	tren	0	$C2/c$	[11b]
	$[M(tepa)]_2(\mu_2\text{-}Sn_2Se_6)$ (M = Fe(57), Co(58), Mn(59))	MCl_2 (or Fe) + $SnCl_4 + Se$	tepa + H_2O	0	$I4_1/a$	[13d,13e]
	$[Mn(tepa)]_2(\mu_2\text{-}Sn_2S_6)$(60)	$MnCl_2 + SnCl_4 + S$	tepa + H_2O	0	$I4_1/a$	[13e]
	$\{Mn(tren)\}_2(\mu_2\text{-}Sn_2Se_6)$(61)	$Mn + Sb + Se$	tren	0	$P\bar{1}$	[27a]
	$[\{Mn(terpy)\}_2(\mu\text{-}Sn_2Se_6)]$(62)	$[MnCl_2(terpy)] + Sn + Se + Cs_2CO_3$	H_2O + en	0	$P\bar{1}$	[27b]
	$[\{Mn(terpy)\}_2(\mu\text{-}Sn_2Se_6)]_n$(63)	$[MnCl_2(terpy)] + Sn + Se + Cs_2CO_3$	H_2O + en	1	$P\bar{1}$	[27b]
	$[\{Mn(cyclam)\}_2(\mu\text{-}Ge_2Se_7)]CH_3OH{\cdot}1.5H_2O$(64)	$[MnCl_2(cyclam)]Cl + GeSe_2 + Na_2CO_3$	$CH_3OH + H_2O$	0	$P2_1/n$	[27b]
	$[\{Mn(cyclam)\}_2(\mu\text{-}Sn_2Se_{6.15})]$(65)	$[MnCl_2(cyclam)]Cl + SnSe + Se + Cs_2CO_3$	$CH_3OH + H_2O$	0	$P2_1/n$	[27b]
	$[Mn(tepa){\cdot}Sn_3Se_7]_n$(66)	$MnCl_2 + SnCl_4 + Se$	tepa + H_2O	1	$P2_12_12_1$	[13e]
	$[\{Mn(en)_2\}_2(\mu\text{-}en)(\mu\text{-}Sn_2S_6)]_n$(67)	$MnCl_2 + SnCl_4 + S$	en/two-step reaction	1	$P\bar{1}$	[13i]
	$[Na(H_2O)_3][Cr(en)_3]_2[GeS_3(OH)]_2[Cr(en)_2(GeS_4)]$(68)	$[Cr(en)_3]Cl_3 + Na_4[GeS_4]$	H_2O	0	$C2/c$	[28]
	$[K_6(MeOH)_9][Sn_2Se_6][Cr(en)_2(SnSe_4)]$(69)	$[Cr(en)Cl_2]Cl + K_4[SnSe_4]$	CH_3OH	0	$P\bar{1}$	[28]
	$[Ba(H_2O)_9][\{Cr(en)\}_2(GeSe_4)_2]$(70)	$[Cr(en)_2Cl_2]Cl + [Ba_2(H_2O)_9][GeSe_4]$	H_2O	0	$P\bar{1}$	[28]
	$[Mn(teta)(en)]{\cdot}[Mn(teta)][Mn(SnTe_4)_2{\cdot}Mn(teta)]$(71)	$Sn + Mn + Te$	teta	1	$P2_12_12_1$	[12]

[a] The number in parentheses after space group (*) is the compound number to distinguish the compounds which have the same chemical formular but different space group.

Table 3
Preparative information for the chalcogenometalates of Group 15 elements with amine complexes

	Compounds	Reactants	Solvent	Space group	*d*	Reference
Anion with discrete complex cation	$[Cr(en)_3][SbS_4](72)$	$CrCl_3{\cdot}8H_2O + Sb_2S_3 + S$	en + H_2O	$P4_2bc$	0	[10b]
	$Ln(en)_4][SbS_4]{\cdot}0.5en$ (Ln = Eu(73), Dy(74), Yb(75), Sm(76), Gd(77))	$Ln_2O_3 + Sb + S$	en	$P2_1/n$	0	[14c,14d,14e]
	$[Ni(en)_3(Hen)][SbS_4](78)$	$NiCl_2 + Sb + S$	en	$P\bar{1}$	0	[13j]
	$[Ni(en)_3]_2[SbS_4](NO_3)(79)$	$Ni(NO_3)_2 + Sb + S$	en	$I\text{-}4$	0	[29]
	$[Ni(dien)_2]_3[SbS_4]_2(80)$	$Ni + Sb + S$	dien	$P\bar{1}$	0	[30]
	$[M(en)_3(Hen)][SbSe_4]$ (M = Fe(81), Co(82), Ni(83), Mn(84))	$MCl_2 + K_2Se + SbCl_3$ (or $MCl_2 + Sb + Se$)	en	$P\bar{1}$	0	[10e,31]
	$[Sm(en)_4][SbSe_4]{\cdot}0.5en(85)$	$SmCl_3 + Sb + Se$	en	$P2_1/n$	0	[14f]
	$[Fe(en)_3]_2[Sb_2S_5]{\cdot}0.55H_2O(86)$	$Sb_2S_3 + FeCl_2{\cdot}4H_2O + S$	en	$Pca2_1$	0	[32]
	$[Mn(en)_3]_2[Sb_2S_5](87)$	$MnCl_2 + Sb + S$	en	$P2_12_12_1$	0	[13j]
	$[Ni(dien)_2]_2[Sb_2Se_5](88)$	$NiCl_2 + Sb + Se$	dien	$P2_1/n$	0	[33]
	$[Fe(en)_3]_2[Sb_2Se_5](89)$	$Rb_2Se + FeCl_2 + SbCl_3 + Se$	en	$Pbca$	0	[34]
	$[Ni(dap)_3]_2[Sb_2Se_5]{\cdot}2H_2O(90)$	$NiCl_2{\cdot}6H_2O + Sb + Se$	dap + H_2O	$P3_12_1$	0	[13o]
	$[Zn(dap)_3]_2[Sb_2Se_5](91)$	$ZnCl_2{\cdot}6H_2O + Sb + Se$	dap + H_2O	$P2_1$	0	[13o]
	$[M(en)_3]_2[As_2S_5]$ (M = Mn(92), Ni(93))	$MCl_2 + As_2O_3 + S$	en	$P2_12_12_1$(92); $Pbca$(93)	0	[13k]
	$[M(en)_3]_2[As_2Se_5]$ (M = Mn(94), Co(95))	$MCl_2 + As_2O_3 + Se$	en	$Pbca$	0	[13k,35]
	$[M(en)_3][As_2Se_6]$ (M = Fe(96), Mn(97))	$M + As + Se$	en	$C2/c$	0	[36]
	$[Mn(dien)_2]_3[As_3Se_6]_2(98)$	$M + As + Se$	dien	$P2_1/c$	0	[36]
	$[Co(dien)_2]_2[Sb_2Se_6](99)$	$CoCl_2 + + Sb + Se$	dien	$P2_1$	0	[33]
	$[Ni(dien)_2]_3[Sb_3S_6]_2(100)$	$Ni(Ac)_2{\cdot}4H_2O + Sb + S$	dien	$P\bar{1}$	0	[10a]
	$[M(en)_3][Sb_2S_4]$ (M = Co(101), Ni(102))	$NiCl_2$ (or $CoBr_2$) + Na_3SbS_3	en + H_2O	$P2_1/c$	1	[37]
	$[Ni(dien)_2[Sb_4S_8](103)$	$Ni + Sb + S$	dien	$P\bar{1}$	0	[10c]
	$[Fe(en)_3]_2[Sb_4S_8](104)$	$Sb_2S_3 + FeCl_2{\cdot}4H_2O + S$	en	$P2_1/c$	1	[32]
	$[Co(en)_3][Sb_4S_7](105)$	$CoS + Sb_2S_3$	en	$P2_1/c$	1	[38]
	$[Mn(en)_3][Sb_4S_7](106)$	$Mn + Sb$	en	$P2_1/c$	1	[39]
	$[M(en)_3][Sb_4S_7]$ (M = Fe(107), Ni(108))	$NiCl_2$ (or $CoBr_2$) + Na_3SbS_3	en + H_2O	$P2_1/c$	1	[37]
	$[M(dap)_3][Sb_4S_7]$ (M = Ni(109), Co(110))	NiS (or Co) + Sb + S	dap + H_2O	$P2_1/n$	2	[13l]
	$[Ni(dien)_2][Sb_4S_7]{\cdot}H_2O(111)$	$Ni + Sb + S$	dien + H_2O	$P2_1/c$	2	[40a]
	$[Fe(dien)_2][Sb_4S_7]{\cdot}H_2O(112)$	$SnSb_2S_4 + Fe$	dien + H_2O	$P2_1/c$	2	[40b]
	$[Co(dien)_2][Sb_4S_7]{\cdot}0.5H_2O(113)$	$SnSb_2S_4 + Co$	dien + H_2O	$P2_1/c$	2	[40b]
	$[Ni(dien)(tren)]]Sb_4S_7(114)$	$Ni + Sb + S$	dien + tren	$P2_1/n$	2	[40b]
	$[Ni(cyclam)][Sb_4S_7](115)$	$NiSO_4{\cdot}7H_2O + Sb_2S_3 + S$	cyclam + H_2O	$C2/c$	3	[41]
	$[Co(cyclam)]_x[cyclam]_{1-x}[Sb_4S_7]$ $(x \approx 1/3)(116)$	$Co(Ac)_2 + Sb_2S_3 + S$	cyclam + H_2O	$C2/c$	3	[41]
	$[Ni(dien)_2]_2[Sb_4S_9](117)$	$Ni + Sb + S$	dien + H_2O	$P2_1/c$	1	[42]
	$[M(dien)_2]_2[Sb_4Se_9]$ [M = Mn(118), Fe(119)]	$MCl_2 + Sb + Se$	dien	$P2_12_12_1$(118); $P2_1/c$(119)	1	[33]
	$[Co(en)_3][CoSb_4S_8](120)$	$CoBr_2 + Na_3SbS_3$	en + H_2O	$C2$	2	[9]
	$[Fe(dien)_2][Fe_2Sb_4S_{10}](121)$	$Sb + S + FeCl_3$	dien + H_2O	$P\bar{1}$	1	[43]
	$[Fe(dien)_2][Sb_6S_{10}]{\cdot}0.5H_2O(122)$	$Fe + Sb + S$	dien	$C2/c$	2	[44]
	$[Co(en)_3][Sb_{12}S_{19}](123)$	$Sb_2S_3 + CoS + S$	en	$P2_1/c$	3	[10d]
	$[Ni(dien)_2]_3[Sb_{12}S_{21}]{\cdot}H_2O(124)$	$Ni + Sb + S$	dien + H_2O	$C2/c$	3	[40]
	$[Ni(dien)_2]_9[Sb_{22}S_{42}]{\cdot}0.5H_2O(125)$	$Ni + Sb + S$	dien + H_2O	$P\bar{1}$	2	[45]
Covalently linked cations and anions	$[Cr(en)_2SbS_3](126)$	$CrCl_3{\cdot}8H_2O + Sb_2S_3 + S$	en + H_2O	$P2_1/c$	0	[10b]
	$[Cr(teta)(SbS_3)](127)$	$CrCl_3{\cdot}6H_2O + Sb_2S_3 + S$	tren + H_2O	$Pcab$	0	[46]
	$[La(en)_3(\mu_3\text{-}SbS_4)](128)$	$La_2O_3 + Sb + S$	en	$P2_1/c$	1	[14c]
	$[Ln(en)_3(H_2O)(\mu_2\text{-}SbS_4)]$(Ln = Nd(129), Sm(130), Pr(131))	$Ln_2O_3 + Sb + S$	en	$Pnma$	1	[14c,14d,14e]
	$[Mn(tren)(trenH)]SbS_4(132)$	$Mn + Sb + S$	tren	$P\bar{1}$	0	[47]
	$[Mn(chxn)_3]_2[Mn(chxn)_2\text{-}(SbS_4)_2]{\cdot}6H_2O(133)$	$Mn + Sb + S$	tren	$C2/c$	1	[47]
	$[Mn(en)_3][Mn_2(SbSe_4)_2(en)_4\text{-}(H_2O)](134)$	$Mn(Ac)_2{\cdot}4H_2O + CsCl + Sb + Se$	CH_3OH + en	$P2/n$	0	[48]
	$[Mn(en)_3][\{Mn(en)_2(H_2O)\}_2(\mu\text{-}SbSe_4)]\text{-}[Mn(\mu\text{-}SbSe_4)(en)_2]Cl_2(135)$	$Mn(Ac)_2{\cdot}4H_2O + CsCl + Sb + Se$	CH_3OH + en	$P\bar{1}$	1	[48]
	$[Mn(en)_3]_2[Mn_4(en)_9(SbSe_4)_4]{\cdot}2H_2O(136)$	$Mn + Sb + Se$	en + $C_2H_5NH_2$	$P2/n$	1	[49]
	$[Ln(en)_4(SbSe_4)]$ (Ln = La(137), Nd(138))	$LnCl_3 + Sb + Se$	en	$P2_1/n$	0	[14f]
	$[Ln(dien)_2(\mu_3\text{-}AsSe_4)]$ (Ln = Nd(139), Sm(140))	$Nd_2O_3 + As_2O_3 + Se$	dien	Iba_2(139); $Pbca$(140)	1	[14i]
	$[Mn(tren)Sb_2S_4](141)$	$Mn + Sb + S$	tren + H_2O	$P2_1/c$	1	[50]
	$[Mn(tren)Sb_2S_4](142)$	$Mn + Sb + S$	tren + H_2O	$C2/c$	1	[50]
	$[Co(tren)Sb_2S_4](143)$	$Co + Sb + S$	tren + H_2O	$Pbca$	2	[51]
	$[Ni(tren)Sb_2S_4](144)$	$Ni + Sb + S$	tren + H_2O	$P2_1/n$	1	[51]
	$[\{Mn(tren)\}(As_2Se_4)](145)$	$[MnCl_2(tren)] + Se + As + Cs_2CO_3$	tren + H_2O	$P2_12_12_1$	1	[52]
	$[\{Mn(terpy)\}_2(As_2Se_4)]{\cdot}2H_2O(146)$	$[MnCl_2(terpy)] + Se + As + Cs_2CO_3$	tren + H_2O	$P2_1/n$	0	[53]
	$\{[Mn(tren)]_2(Sb_2S_5)\}(147)$	$Mn + Sb + S$	tren + H_2O	$Pbcn$	0	[54]
	$\{[Co(tren)]_2(Sb_2S_5)\}(148)$	$Co + Sb + S$	tren	$C2/c$	0	[55]
	$\{Mn_2(dape)(Sb_2S_5)\}(149)$	$Mn + Sb + S$	dape	$Pbca$	2	[56]
	$\{Mn_2(dap)(Sb_2S_5)\}(150)$	$Mn + Sb + S$	dap		2	[57]
	$\{Mn_2(dien)(Sb_2S_5)\}(151)$	$Mn + Sb + S$	dien	$P2_1/c$	2	[58]
	$\{Mn_2(mdap)(Sb_2S_5)\}(152)$	$Mn + Sb + S$	mdap	$P2_1/$	2	[58]
	$\{Mn_2(en)(Sb_2S_5)\}(153)$	$Mn + Sb + S$	en	$P\bar{1}$	1	[59]

Table 3 (*Continued*)

Compounds	Reactants	Solvent	Space group	*d*	Reference
$[\{Mn(tren)\}_2(As_2Se_5)]\cdot 0.5H_2O$(154)	$[MnCl_2(tren)] + Se + As + Cs_2CO_3$	$tren + H_2O$	$P\bar{1}$	0	[53]
$[\{Mn(tren)\}_2(As_2Se_6)_2]$(155)	$[MnCl_2(tren)] + Se + As + Cs_2CO_3$	$tren + H_2O$	$P\bar{1}$	0	[53]
$\{[Zn(tren)]_2Sb_4S_8\}\cdot 0.75H_2O$(156)	Zn + Sb + S	tren	$P2_1/c$	0	[60]
$\{[Co(tren)]_2Sb_4S_8\}$(157)	Co + Sb + S	tren	$P2_1/c$	0	[55]
$\{[M(tren)]Sb_4S_7\}$ (M = Mn(158), Fe(159), Co(160), Zn(161))	M (or $FeCl_3$) + Sb + S	$tren + H_2O$	$P2_1/n$	1	[61]
$[Ni(tren)]Sb_4S_7$(162)	Ni + Sb + S + Sn	tren	$P\bar{1}$	1	[40b]
$[\{Mn(tren)\}(As_4Se_7)]$(163)	$[MnCl_2(tren)] + Se + As + Cs_2CO_3$	$tren + H_2O$	$P\bar{1}$	1	[52]
$[M(teta)]Sb_4S_7$ (M = Zn(164), Mn(165))	M + Sb + S	Teta	$P\bar{1}$	1	[40b]
$\{[Fe(tren)](FeSbS_4)\}$(166)	$Sb + S + FeCl_3$	$tren + H_2O$	$P\bar{1}$	2	[43]
$\{[Mn(tren)]_4(Mn_2Sb_4S_{12})\}$(167)	Mn + Sb + S	$tren + H_2O$	$P\bar{1}$	0	[62]
$\{[Mn(tren)]_2(Mn_2Sb_4S_{10})\}$(168)	Mn + Sb + S	$tren + H_2O$	$P\bar{1}$	1	[54]
$[Mn(dien)_2]_n[Mn(dien)AsS_4]_{2n}\cdot 4nH_2O$(169)	Mn + As + S	dien	$P2_1/c$	1	[63a]
$[Mn(en)_3]_2[Mn(en)_2AsS_4][As_3S_6]$(170)	Mn + As + S	en	*Cc*	0	[63a]
$[Mn_3(2,2'\text{-bipy})_3(As^VS_4)_2]_n\cdot nH_2O$(171)	$MnCO_3 + As + S + 2,2'$-bipy	H_2O	*Pbcn*	1	[63b]
$Mn_2(2,2'\text{-bipy})As_2{}^{III}S_5$(172)	$MnCO_3 + As + S + 2,2'$-bipy	$dien + H_2O$	$P2_1/c$	2	[63b]

Table 4
Physical constants for chelating organic amines

	en	dap	dien	teta	tepa
Molecular formula	$C_2H_8N_2$	$C_3H_{10}N_2$	$C_4H_{13}N_3$	$C_6H_{18}N_4$	$C_8H_{23}N_5$
Formula weight ($g\,mol^{-1}$)	60.10	74.13	103.17	146.24	189.30
Melting point (°C)	8.5	−37.2	−39	12	−30
Boiling point (°C)	117.3	120.9	206.7	267	333
Flash point (°C)	43	33.3	101.7	143	163
Density ($g\,cm^{-3}$)	0.8977	0.8732	0.9586	0.9818	0.9980
Refractive index	1.4568^{20}	1.4460^{20}	1.4844^{20}	1.4971^{20}	1.5042^{20}
Viscosity (η, $mN\,s\,m^{-2}$)	1.54 (20 °C)	1.70(20 °C)	7.1(20 °C)	–	–
Dielectric constant (ε)	14.2 (20 °C)	–	12.63(20 °C)	–	9.40
Solubility	misc-w, al	misc-w, al	misc-w, al	misc-w, al	misc-w, al

Misc: Miscible, w: water, al: ethanol.

en)]$^{6+}$ [25] and $[Zn(tren)(\mu\text{-teta})_{0.5}]^{2+}$ [13b]. The structure of the $[Nd_2(en)_6(\mu_2\text{-OH})_2]^{4+}$ ion is shown in Fig. 3a. Two $[Nd(en)_3]$ moieties are joined by two μ_2-OH bridging groups to form a centrosymmetric dimer. There are three types of coordinated en molecules in the dinuclear $[\{Mn(en)_2(enH)\}_2(\mu\text{-en})]^{6+}$ cation (Fig. 3b), in which the mono-coordinated en is an unusual one. In the $[\{Zn(tren)\}_2(\mu\text{-teta})]^{4+}$ cation, the amine bridge is tren molecule connected by the *trans*-terminal N atoms (Fig. 3c). The tren molecule found in related coordination compounds usually acts as a strong chelate ligand [11b,50,54], therefore, the linear bridging coordination of tren is a relatively rare example within the chalcogenidometalate chemistry.

The chelating organic amines coordinate to metal ions forming metal complexes that can combine hydrophilic with hydrophobic structure-directing effects, namely its positive charge favors the formation of the charged and generally hydrophilic framework, while its hydrophobic carbon backbone group tends to favor the more hydrophobic organic surface on the cation's assembly. Such an 'amphiphilic' structure-directing effect may play a role in the formation of various new structures. The metal complex cations can assemble to form pseudo-channels, enwraping the linear chalcogenidometalate anions, which is denoted as 'outside template effect'. For example, the organic amine groups of the $[La(en)_4Cl]^{2+}$ cation [15] are arranged in four orientations (Fig. 4a). The pseudo

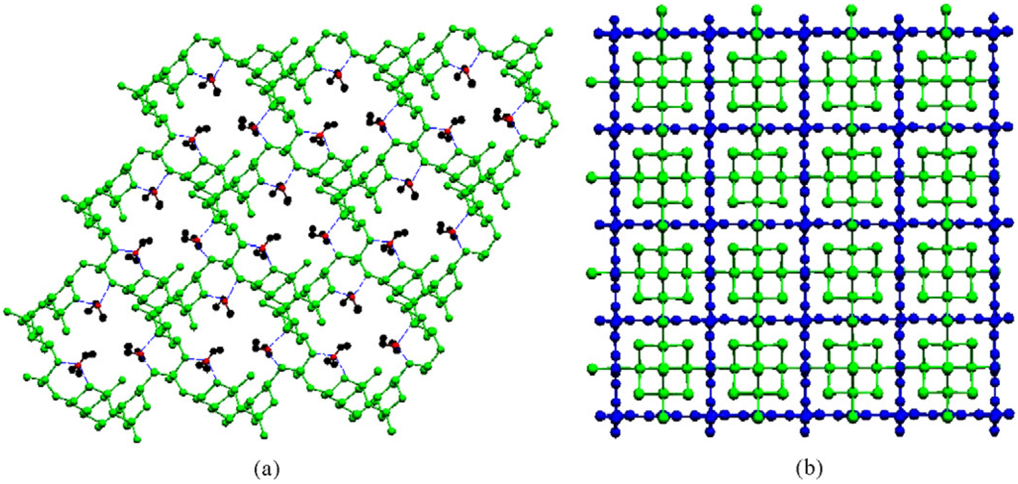

Fig. 1. (a) The $[(C_2H_5)_2NH_2]^+$ cations in $[(C_2H_5)_2NH_2]_7[In_{11}S_{21}H_2]$ [6f] are located in the pores of the layer. (b) The structure-directing agents (H_2dap cations) in $[H_2dap]_2[Ga_4Se_8]$ [13c] are arranged in a band-like structure, which resides above the grooves of the layer.

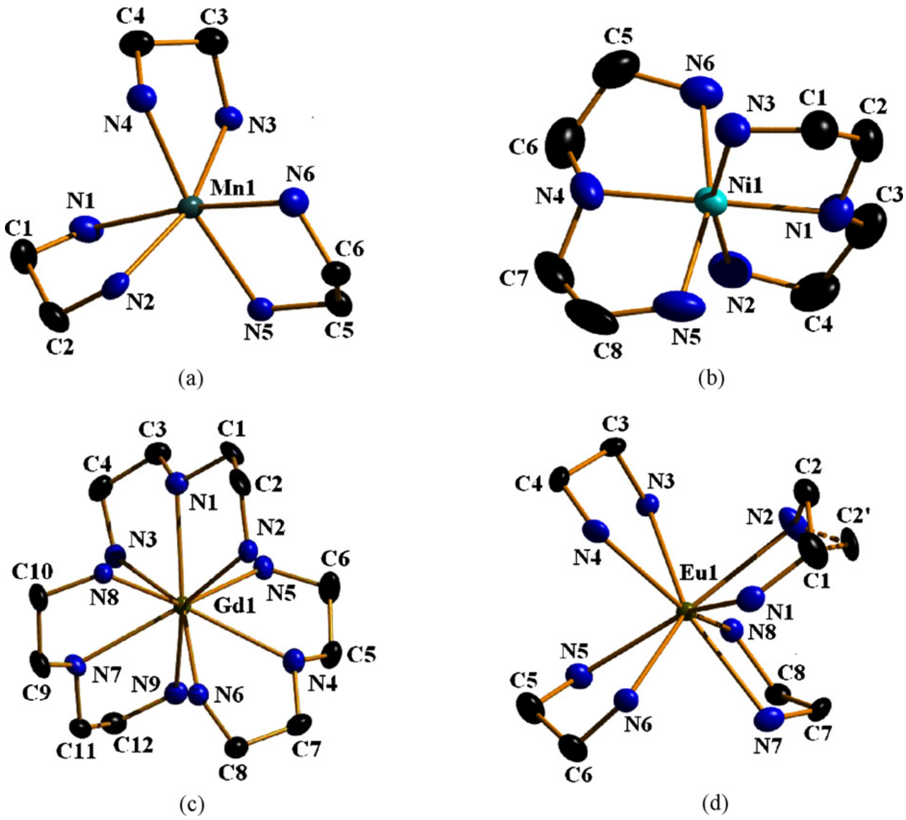

Fig. 2. The mono-nuclear complex cations: (a) $[Mn(en)_3]^{2+}$ ion in $Mn(en)_3]_2[Sn_2S_6]$(25) [13f], (b) $[Ni(dien)_2]^{2+}$ ion in $[Ni(dien)_2][Sb_4S_7]{\cdot}H_2O$(111) [40a], (c) $[Gd(dien)_3]^{3+}$ ion in $[Gd(dien)_3]_2[(Sn_2S_6)Cl_2]$(35) [14b] and (d) $[Eu(en)_4]^{3+}$ ion in $Eu(en)_4][SbS_4]{\cdot}0.5en$(73) [14c].

rectangular channels are constructed by the complex cations surrounding the 1D $[InTe_2]^-$ chains. But the organic amine groups of $[Ni(en)_3]^{2+}$ [13b] are arranged in three orientations (Fig. 4b), the pseudo-hexagonal channels are built from the complex cations and free en molecules via H-bonding. On the other hand, the guest metal complex cations are similar to nonchelating organic amine cations located in the pores or channels of the host chalcogenidometalate anion, which can be denoted as 'inside template effect'. For instance, the $[Ni(dap)_3]^{2+}$ cations in $[Ni(dap)_3][Sb_4S_7]$ [13l] are located in the apertures of the large $Sb_{16}S_{16}$ hetero-rings within the 2D layers

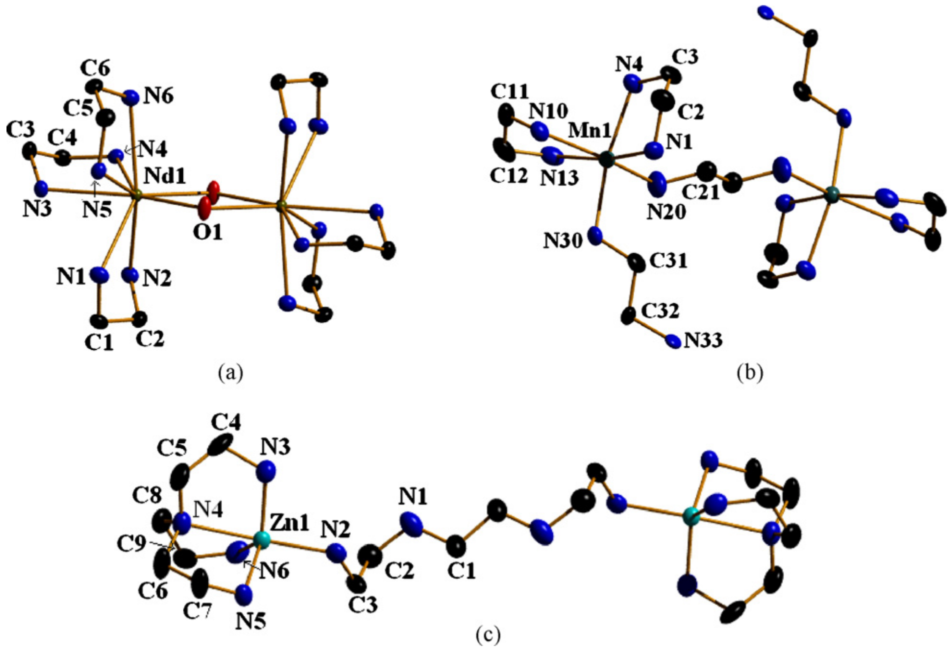

Fig. 3. The dinuclear complex cations: (a) $\{[Nd(en)_3(OH)]_2\}^{4+}$ ion in $[Nd_2(en)_6(\mu_2\text{-}OH)_2][Sn_2S_6]$(33) [14b], (b) $[\{Mn(en)_2(enH)\}_2(\mu\text{-}en)]^{6+}$ ion in $(enH_2)[\{Mn(en)_2(enH)\}_2(\mu\text{-}en)](Ge_2Se_7)_2$(52) [25] and (c) $[\{Zn(tren)\}_2(\mu\text{-}teta)]^{4+}$ ion in $[Zn(tren)(\mu\text{-}teta)_{0.5}][InTe_2]Cl$(9) [13b].

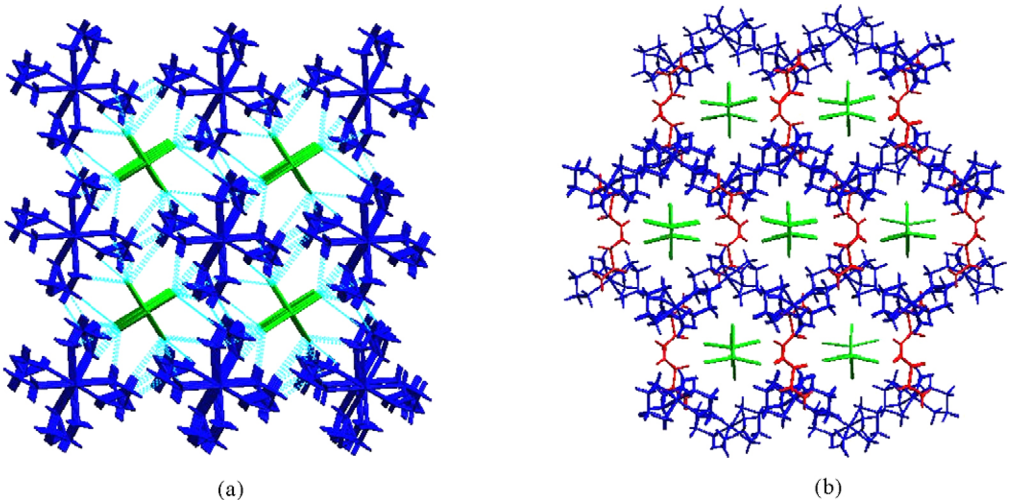
(a) (b)

Fig. 4. Hydrogen-bonding assembled 1D channels $[La(en)_4Cl]^{2+}$ [15] (a) and en/$[Ni(en)_3]^{2+}$ [13b] (b), in which the anionic chains are located.

(Fig. 5a). The $[Co(en)_3]^{2+}$ cations in $[Co(en)_3][Sb_{12}S_{19}]$ [10d] reside in the channels of the $[Sb_{12}S_{19}]^{2-}$ framework (Fig. 5b).

In addition, due to the larger size in radii, complex cation compensates well with the large chalcogenide anion, which accelerates the crystallization. For instance, when incorporation of transition-metals ion into the GeO_2/S_8/en system [13h] under the solvothermal conditions $[M(en)_3]_2Ge_2S_6$ ($M = Mn^{2+}$, Ni^{2+}) were obtained immediately at the end of the solvothermal reaction, When the above reaction system reacted in the absence of M^{2+}, the protonated compound of $(enH)_4Ge_2S_6$ was isolated after the resulted reaction solution was laid aside for 2 weeks at room temperature. The same phenomenon was also found for $SnCl_4/S_8$/en system [13g]. The finding indicates that the solution with complex cation is easy to be supersaturated, so that crystallization of the product can immediately occur.

2.4. Properties and structural influences of the unsaturated complex cations

The chelating amine ligands were used in the synthesis that cannot complete the coordination sphere of the transition metal ion, resulting in the unsaturated complex cation. The unsaturated complex cations are able to form bond(s) to the chalcogenidometalate anions, for which a great diversity of structures can be expected. For instance, Bensch et al. and Powell and co-workers prepared a series of thioantimonates(III), such as $[Cr(teta)(SbS_3)]$ [46], $\{[Mn(tren)]_4(Mn_2Sb_4S_{12})\}$ [62], $\{[Mn(tren)]_2(Mn_2Sb_4S_{10})\}$ [54], and two thiostannates(IV) $[M(tren)_2]_2(\mu\text{-}Sn_2S_6)$ (M = Ni, Co) [11b] in the presence of tetradentate tris(2-aminoethyl)amine (or triethylenetetramine). Whether the chalcogenidometalate anion acts as a ligand to the metal center of a complex cation depends on the coordination number of the chelating amines and the synthetic conditions. Usually, tetra- or pentadentate amines, or lanthanide ions have been used to form a complex cation with an unsaturated coordination sphere, such as $[M(tren)]^{2+}$ (M = Co, Ni) [11b], $[M(tepa)]^{2+}$(M = Fe, Co, Mn) [13d,e] and $[Ln(en)_3(H_2O)]^{3+}$ (Ln = Nd, Sm, Pr) [14c–e]. Recently, our group has successfully obtained two thiogallates $\{[Ni(tepa)]_2SO_4\}$ $[Ni(tepa)(Ga_4S_6(SH)_4)]$ and $\{[Mn(atep)](Ga_2S_4)\}$ [13c], one thioindate $[Ni(tepa)]_2[In_4S_7(SH)_2]\cdot H_2O$ [13a], a series of selenidostannate(IV), for example, $[M(tepa)]_2(\mu_2\text{-}Sn_2Se_6)$ (M = Mn, Fe, Co) [13d,e] and $[Mn(tepa)\cdot Sn_3Se_7]_n$ [13e]), and chalcogenidoantimonates(III), such as $[Ln(en)_3(H_2O)$ $(\mu_2\text{-}SbS_4)]$ (Ln = Nd, Sm, Pr) [14c–e] and $[Ln(en)_4(SbSe_4)]$ (Ln = La, Nd) [14f], using this strategy. In addition, Mn^{2+} ion seems to behave very different to Ni^{2+}, Co^{2+}, Zn^{2+} and Fe^{3+}. It has a more or less identical affinity to N and S, and it is not necessary to use such multidentate amines that not fully saturate the coordination sphere, which is evidenced by the $[Mn_2(L)(Sb_2S_5)]$ family with L = 1,3-diaminopentane, diaminopropane, diethylen-

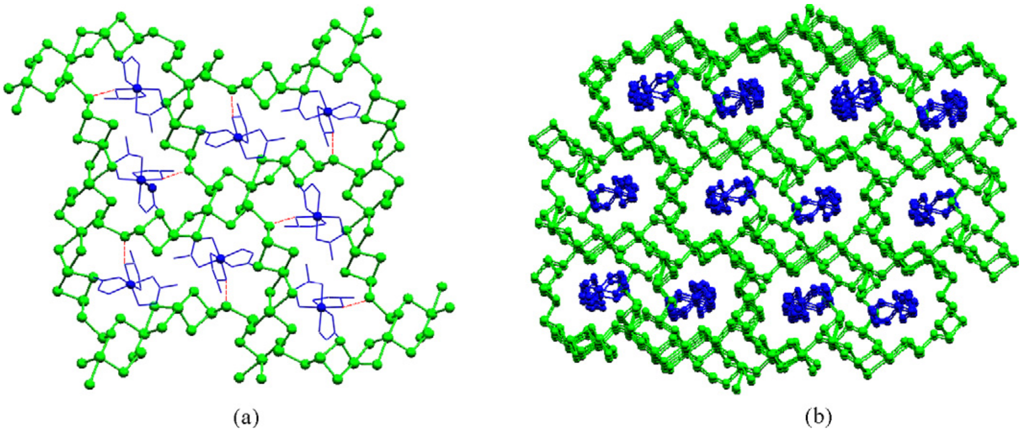
(a) (b)

Fig. 5. (a) The $[Ni(dap)_3]^{2+}$ cations are located in the pores of the $[Sb_4S_7]^{2-}$ framework [13l]. (b) The $[Co(en)_3]^{2+}$ cations are located in the one-dimensional channels of the $[Sb_{12}S_{19}]^{2-}$ framework [10d].

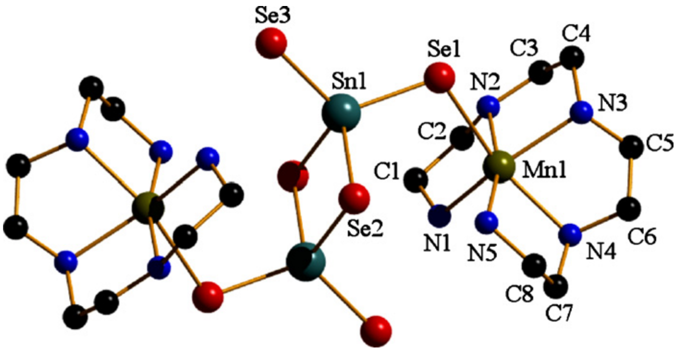

Fig. 6. Crystal structure of $[Mn(tepa)]_2(\mu_2\text{-}Sn_2Se_6)$(59) [13e].

etriamine, N-metyl-1,3-diaminopropane, or ethylenediamine [56–59].

The unsaturated metal complex subunits may bond directly to the chalcogenidometalate skeletal core as decorating groups, bridging groups or structure directing groups. The bonded metal complexes contribute to the increased complexity and functionality of the chalcogenide by assimilation as one component in a hierarchical structure where there is a synergistic interaction between the metal complex and the inorganic chalcogenide. As shown in Fig. 6, the $[Sn_2Se_6]^{4-}$ anion in $[Mn(tepa)]_2(\mu_2\text{-}Sn_2Se_6)$(59) [13e], located at a center of inversion, connects two $[Mn(tepa)]^{2+}$ terminating groups by the trans terminal Se atoms to form a neutral compound. While $[Mn(tepa)\cdot Sn_3Se_7]_n$ [13e] is an example that the metal complex displays structure-decorating role (Fig. 7). The structure of $[(C_3H_7)_3NH]_2Sn_3Se_7$ [6a] contains a 1D $[Sn_3Se_7]^{2-}$ chain constructed by trinuclear Sn_3Se_4 semi-cube cluster (Fig. 7a). When this chain is decorated by the unsaturated complex $[Mn(tepa)]^{2-}$, a chiral 1D selenidostannate $[Mn(tepa)\cdot Sn_3Se_7]_n$ chain is formed (Fig. 7b). The negatively charged Mn–Te–Sn helical chains in $[Mn(teta)(en)]\cdot[Mn(teta)][Mn(SnTe_4)_2\cdot Mn(teta)]$ [12] are decorated with pendent metal complexes at the outer surface of the helices (Fig. 8). The chalcogenidometalate anion as ligand coordinates to metal center of the unsaturated metal complex, which may lead to change of the conformation of the chalcogenidometalate. The terminal S atoms in $[Ni(en)_3]Sb_2S_4$(102) [37] are arranged on both sides of the 1D $[SbS_2]^-$ chain built from repeated corner-bridging of $[SbS_3]^{3-}$ trigonal pyramids (Fig. 9a). But after coordination of the terminal S atoms to the metal center of [Ni(tren)] sphere in $[Ni(tren)]Sb_2S_4$(144) [51], one side of the terminal S atoms are rotated to the other side of the 1D $[SbS_2]^-$ chain (Fig. 9b). A similar phenomenon is observed in the $[Sb_2S_5]^{4-}$ anion. The two SbS_3 trigonal pyramids in the discrete $[Sb_2S_5]^{4-}$ anion [13j] are in *cis*-conformation. After two unsaturated $[Co(tren)]^{2+}$ groups are incorporated into the $[Sb_2S_5]^{4-}$ anion in $\{[Co(tren)](Sb_2S_5)\}$(148) [55], the two SbS_3 trigonal pyramids are in *trans*-conformation.

The concept of using metal ion 'nodes' and bridging ligand 'spacers' in the design and synthesis of organic/inorganic hybrid materials has been widely acknowledged by the virtue of advantages over conventional materials [64]. So the design of supramolecular assemblies has led to various supramolecular structures, along with potential applications as functional solid materials [65]. In the organic–inorganic hybrid chalcogenidometalates of Goup 13–15 elements, the unsaturated metal complex also can act as the proposed 'node', showing structure-building functions. As illustrated in Fig. 10, the coordination sphere of Nd^{3+} ion is not completed, and two of the coordination sites of the Nd^{3+} cation can be further coordinated by the sulfur

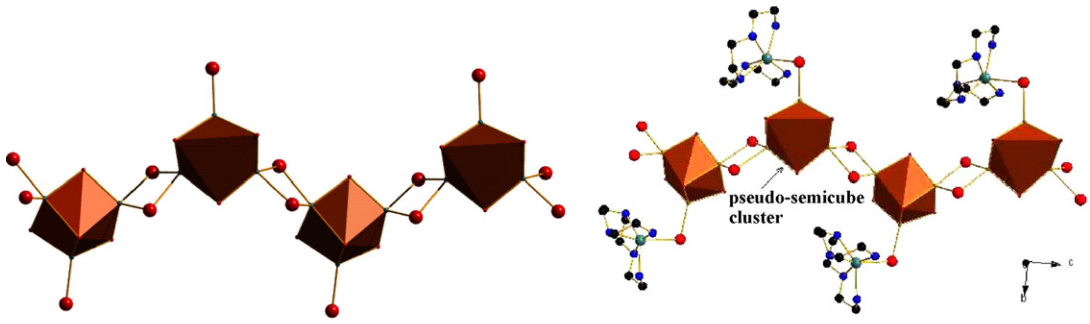

(a) (b)

Fig. 7. (a) 1D $[Sn_3Se_7]^{2-}$ chain in $[(C_3H_7)_3NH]_2[Sn_3Se_7]$ [6a] and (b) 1D chiral $\{[Mn(tepa)]Sn_3Se_7\}_n$ chain [13e].

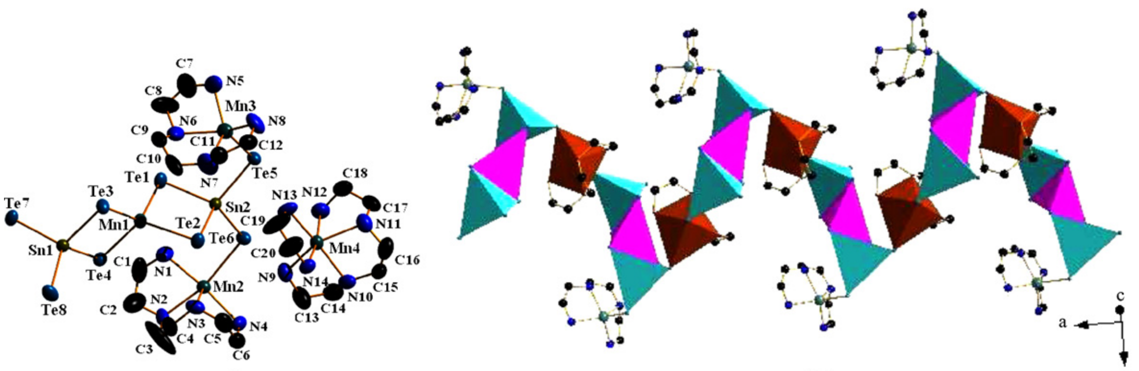

(a) (b)

Fig. 8. (a) Crystal structure of $[Mn(teta)(en)]\cdot[Mn(teta)][Mn(SnTe_4)_2\cdot Mn(teta)]$(71) [12] and (b) 1D helix chain in 71, showing the connection of the polyhedrons.

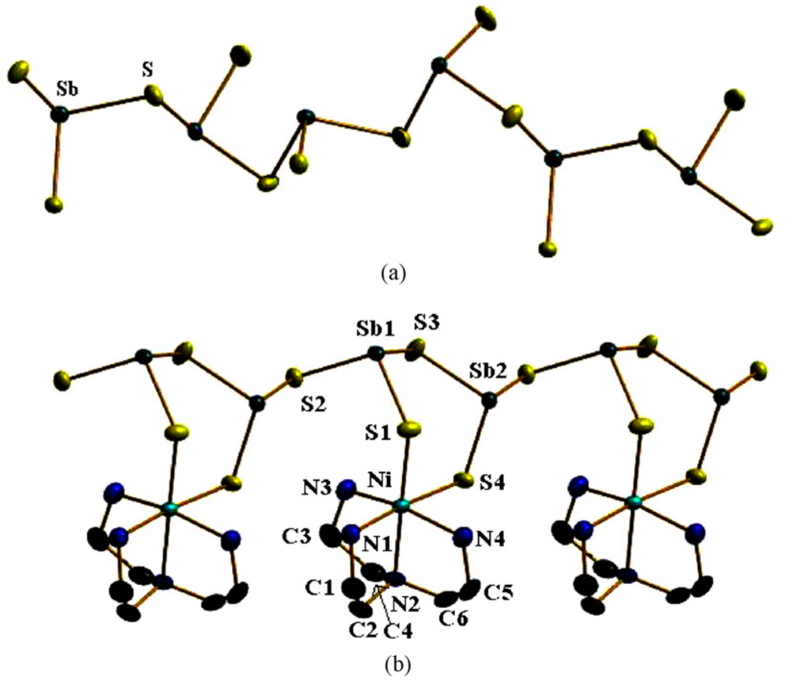

Fig. 9. (a) 1D SbS_2^- chain in $[Ni(en)_3][Sb_2S_4](102)$ [37] and (b) 1D $\{[Ni(tren)]Sb_2S_4\}_n$ chain [51].

atoms of the SbS_4 units [14c]. The $[Nd(en)_3(H_2O)]^{3+}$ fragments (node) are bridged by SbS_4 group (spacer) to forming a neutral one-dimensional $[Nd(en)_3(H_2O)(\mu_2\text{-}SbS_4)]_n$ chain. Besides the inorganic bridging 'spacer', an organic 'spacer' is observed in $[\{Mn(en)_2\}_2(\mu\text{-en})(\mu\text{-}Sn_2S_6)]_n$ [13i]. Two types of bridging 'spacers' are arranged alternately between $[Mn(en)_2]$ fragments (node) (Fig. 11). The inorganic bridging 'spacer' in both examples is linked to the metal complex 'node' by a terminal S atom, while, interestingly, non-terminal S atoms of a polymeric anion coordinating to metal centers has been found in $Mn(en)_2Ga_2S_4$ [11a]. The $[GaS_2]^-$ chains are joined by $[Mn(en)_2]^{2+}$ groups ('node') with the two bridging S atoms from two different $[GaS_2]^-$ chains in a trans arrangement (Fig. 12). These $[Mn(en)_2]^{2+}$ groups serve as the two-connected link to join the $[GaS_2]^-$ chains along the [1 1 0] and [1–10] directions in an alternating fashion, forming a three-dimensional network. The structures of relevant compounds will be elaborated in Section 3.2.

Although transition metal ions with bi- or tri-dentate amines usually prefer a saturate octahedral coordination sphere, in some cases, the complex cations with these amines could be incorporated into a main-group anionic network under certain reaction conditions. Bensch et al. prepared $[Cr(en)_3]SbS_4$ [10b] containg discrete $[Cr(en)_3]^{2+}$ cations with $CrCl_2{\cdot}8H_2O$, Sb_2S_3 and S in a molar ratio of 1:1:3.5 in an aqueous solution of en at 150 °C. But another thioantimonate compound $[Cr(en)_2SbS_3]$ [10b] was obtained by changing molar ratio ($CrCl_2{\cdot}8H_2O/Sb_2S_3/S = 1{:}0.5{:}2.5$) under similar solvothermal conditions, which can be viewed as a mononuclear chromium complex that contains two chelating *en* ligands besides one chelating SbS_3 group. A different synthetic route can also lead to the different compound with the same organic amine. An example is $[Mn(en)_3][Sn_2S_6]$, which was obtained by a one-step solvothermal reaction [13f], but a 1D thiostannate compound, $[\{Mn(en)_2\}_2(\mu\text{-en})(\mu\text{-}Sn_2S_6)]_\infty$ [13i], was synthesized by a two-step solvothermal synthesis.

Transition metal ions like Cu^+, Ag^+, Cd^{2+} and Hg^{2+} are strongly chalcophilic and have little tendency to form complex cations with the amines in the presence of chalcogenide ions, which usually bond directly to the chalcogen elements. Good examples are $(H_2en)[Ag_2SnS_4]$ [66], $(dienH_2)_{0.5}[Cu_2SbS_3]$ [6b], $(dienH)[Cu_3Sb_2S_5]$ [6b], $[trenH_2][Cu_3Sb_2S_5]$ [6b], and $K_2[HgSnTe_4]$ [67], in these compounds the transition-metal cations have been fully incorporated into the main group framework. Their counterions are protonated amines or alkali metal ions. Therefore the structures of these compounds will not be discussed herein.

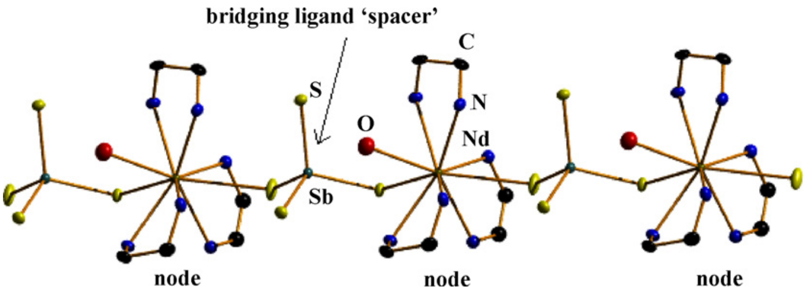

Fig. 10. 1D $[Nd(en)_3(H_2O)(SbS_4)]_n$ chain [14c], showing the 'node' and the 'spacer'.

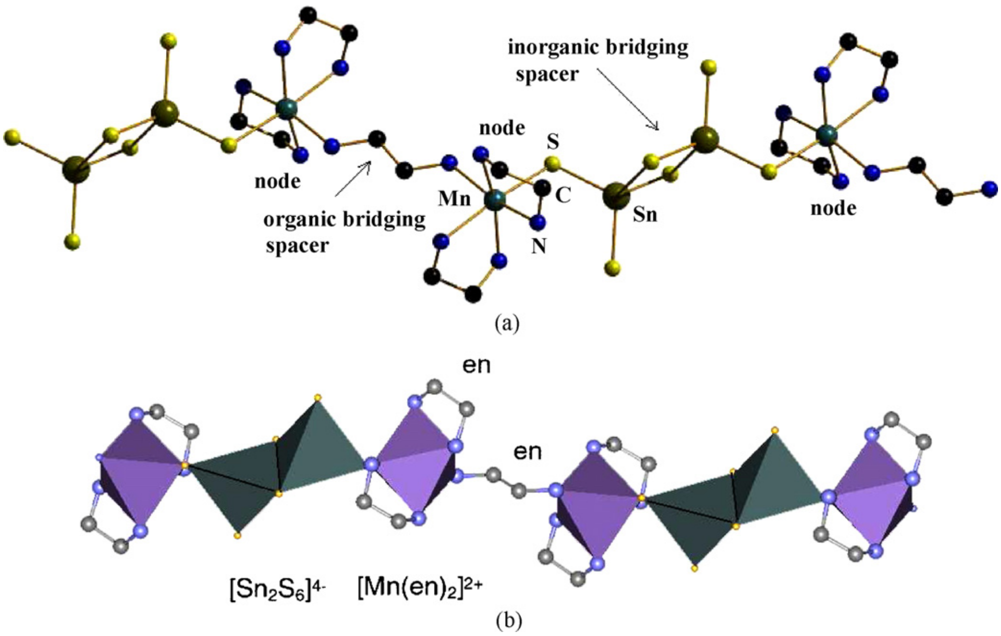

Fig. 11. (a) 1D structure of $[\{Mn(en)_2\}_2(\mu\text{-en})(\mu\text{-}Sn_2S_6)]_n$(67) [13i], showing the 'node' and the 'spacer' (a) and the connection of the polyhedrons (b).

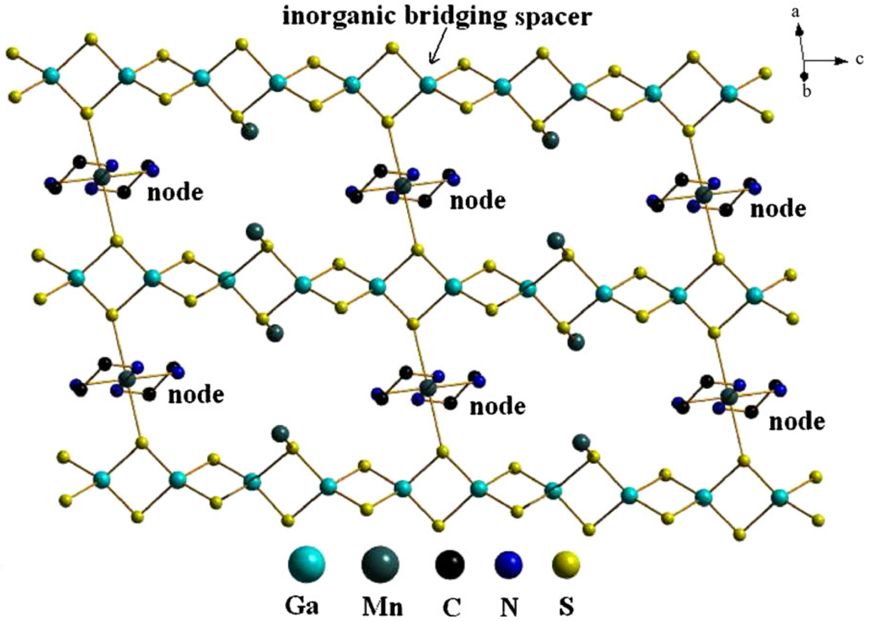

Fig. 12. Part of the crystal structure of $\{Mn(en)_2(Ga_2S_4)\}$(21) [11a], showing the 'node' and the 'spacer'. For the sake of clarity, the inorganic bridging 'spacers' in another direction have been omitted.

3. Structures of Group 13–15 chalcogenidometalates

3.1. Chalcogenidometalates with discrete metal complex cations

These are molecular species of general formula $[M(amine)_x]_yM'_nQ_m$ or $[M(amine)_x]_yM'_nM''_zQ_m$ (M = divalent transition metal, M′ = main Group 13–15 metal, M″ = M or other transition metal) with effective charge separation between complex cations $[M(amine)_x]^{2+}$ and anionic structural units $[M'_nQ_m]^{2y-}$ or $[M'_nM''_zQ_m]^{2y-}$ (charges = 3y for trivalent complex cations). A good relationship between dimensionality of the main group chalcogenidometalate anions and the size of charge balancing counter ion (complex cation) is observed, and the chalcogenidometalates exhibit a greater tendency for the formation of low dimensional structures with increasing size of the cation. In the presence of the larger complex cations as counterions, the anions of chalcogenogallates and—indates generally adopt 1D $[MQ_2]^-$ or $[M_2Q_6]^{2-}$ chain structures, such as $[M(en)_3]_{0.5}[GaS_2]$(M = Mn, Co, Ni) [11a], $[Ni(dien)_2]_{0.5}[InS_2]$ [13a], $[Mn(dap)_3]_{0.5}[GaSe_2]$ [13c], $[M(en)_3][In_2Te_4]\cdot en$ (M = Ni, Co) and $[M(en)_3][In_2Te_6]$ (M = Fe, Zn) [13b], and the only example is the 2D layer $[Zn(en)_3]_4[In_{16}(Te_2)_4(Te_3)Te_{22}]$ [17]. The anions of chalcogenogermanates and—stannates usually present dimeric $[M_2Q_6]^{4-}$ or $[M_2Q_7]^{4-}$ structures (such as $[M(en)_3]_2[Sn_2S_6]$ (M = Mn, Co, Zn, Ni) [13f,g], $[Mn(en)_3]_2[Sn_2Te_6]\cdot 4H_2O$ [22] and $(enH_2)[\{Mn(en)_2(enH)\}_2(\mu\text{-en})](Ge_2Se_7)_2$ [25]), and only 1D

Zintl chain of $[CdSnTe_4]^{2-}$ [24], and two 2D layers including $[Ag_6Sn_2Te_8]^{2-}$ [24] and $[ZnGe_3S_9(H_2O)]^{4-}$ [26]. Compared with the chalcogenido anions of Group 13/14 elements, chalcogenido anions of As and Sb chalcogenides display richer structural moieties which range from tetrahedral $[MQ_4]^{3-}$ [14c–e] to dimeric $[M_2Q_5]^{4-}$ [32–34] or $[M_2Q_6]^{4-}$ [36], oligomeric $[M_3Q_6]^{3-}$ [36], 1D $[M_2Q_4]^{2-}$ [37] or $[M_4Q_x]^{y-}$ ($x = 7$ or 8, $y = 2$; $x = 9$, $y = 4$) [32,38,42] chain structures, and a relatively small number of 2–3D polymeric anionic structures [40,41,44,45].

3.1.1. *Crystal structures of Group 13 chalcogenidometalate (Ga, In) anions*

The most common 1D $\{[MQ_2]^{n-}\}_\infty$ chains (Zweier single chain) constructed by MQ_4 tetrahedra sharing opposite edges have been found in $[M(en)_3]_{0.5}[GaS_2]$ (M = Mn(1), Co(2), Ni(3)) [11a] and $[La(en)_4Cl][In_2Te_4]$(15) [15]. The compounds 1–3 and 15 were synthesized by two different groups in solvothermal synthesis using en as a reaction medium. Examples of such chains have been observed previously in $MInQ_2$ (M = Na, K, Rb, Tl; Q = Te, and M = Tl, Q = Se) [67–70], $TlGaTe_2$ [70], and AIn_2Te_4 (A = Ca, Sr, Ba) [68,71] which are usually obtained by flux growth technique at intermediate or higher temperature. Similar compounds obtained by solventothermal reactions or cathodic dissolution include $[C_{10}N_4H_{26}]_{0.5}[InS_2]$ [72], $[C_{10}N_4H_{26}]_{0.5}[GaS_2]$ [72], $(C_4H_{11}N_2)[GaSe_2]$ [7a], $[(C_4H_9)_4N]_2[In_2Te_4]$ [73] and $(Ph_4P)[GeInTe_4]$ [67], whose counterions are protonated amines, tetra-alkylammonium, or tetraphenylphosphonium ions. In order to learn more about the structural properties of 1D $\{[MQ_2]^{n-}\}_\infty$ chains, we have been successfully prepared a series of analogous 1D chalcogenogallates/indates by using strong chelating organic amines as structure-directing agents. In these studies, 1D $\{[MQ_2]^{n-}\}_\infty$ anionic chains displaying three different types of structural modes were found. The polymeric $\{[MQ_2]^{n-}\}_\infty$ anions in compounds $[Mn(dap)_3]_{0.5}[GaSe_2]$(6) [13c], $[Ni(dap)_3]_{0.5}[InS_2]$(8) [13a] and $[Zn(tren)(\mu\text{-teta})_{0.5}][InTe_2]Cl$(9) [13b] are similar to the aforementioned straight chain (type I) (Figs. 13a and 14a). This type will not be discussed herein in detail, which has been reviewed by Li et al. in [2c]. The binary anions in $[Ni(dien)_2]_{0.5}$ $[InS_2]$(7) [13a] and $[M(en)_3][In_2Te_4]\cdot en$ (M = Ni(10), Co(11)) [13b] represent unusual 1D sinusoidal chains with $[In_4Q_8]^{4-}$ periodic units (Q = S, Te) (type II). Compound 10 is discussed here in detail (Fig. 13b). The repeating sinusoidal unit of type II displays a period of 14.5452(23) Å (In1–In2–In1–In2), which is less than the sum of the four In-In distances (14.6848 Å). The atoms in the In1/Te1/Te2/In2 ring are almost coplanar, while the In1B/Te3/Te4/In2 ring has a

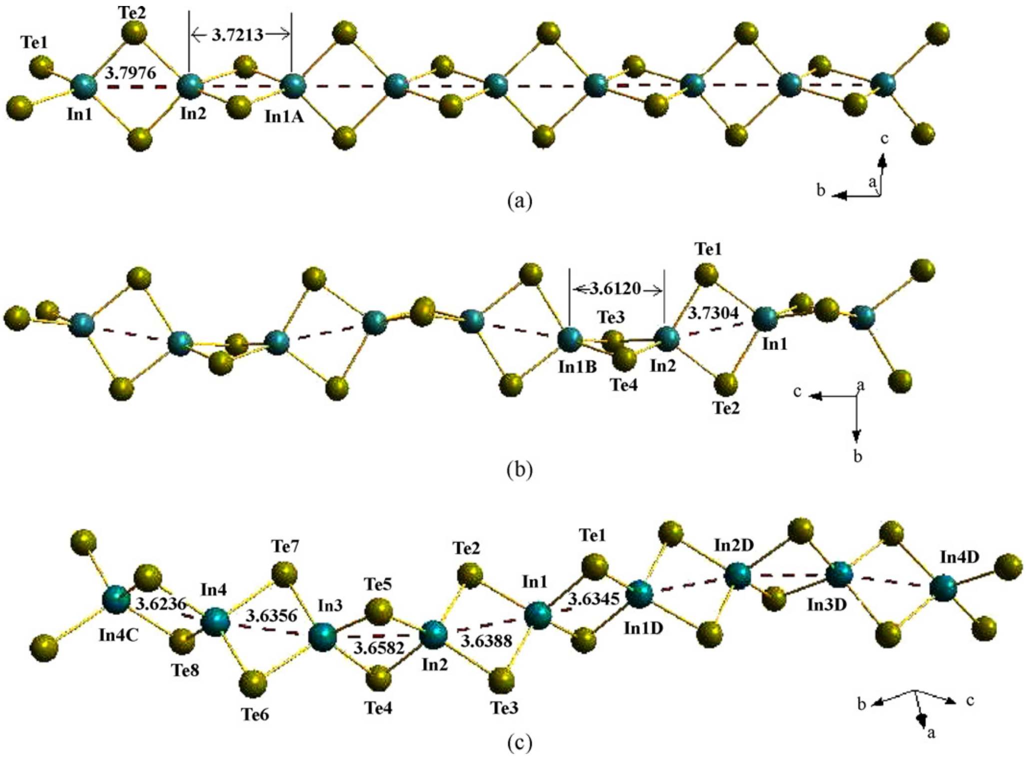

Fig. 13. View of the 1D chains showing the type I structure (a), type II structure (b) and type III structure (c) [13a,b].

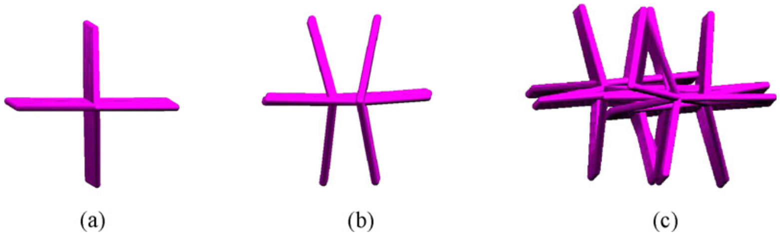
(a) (b) (c)

Fig. 14. The view of the 1D chains along the axial direction, showing the type I (a), type II (b) and type III (c) structures [13a,b].

butterfly structure; the dihedral angle between the wing planes In1B/Te3/In2 and In1B/Te4/In2 is 158.2°. When viewed down the [0 0 1] direction, the In atoms do not form a straight line. Fig. 14b shows the separation of the In atoms and the two alternating orientations of the butterfly rings along the 1D chain axis.

The third type, another novel sinusoidal anionic chain $[In_8Te_{16}{}^{8-}]_n$, is observed in $[M(en)_3]_2\ (en)_{0.5}[In_4Te_8]$ (M = Mn(12), Fe(13), Zn(14)) [13b] (type III). Compound 12 is discussed here in detail (Fig. 13c). The repeating unit of type III is different from that of type I and is similar to that of type II compounds, but it contains eight edge-sharing tetrahedral $[In_8Te_{16}]^{8-}$ those complete a sinusoidal period of 28.4569(37) Å. The In1/Te1/Te1/In1 ring only slightly deviates from a plane while in the perpendicular direction; the In2/Te4/Te5/In3 ring significantly deviates from a plane taking a butterfly shape (Fig. 14c).

The host–guest interactions in the form of electrostatic forces and hydrogen bonding could be related to these different types of 1D $\{[MQ_2]^{n-}\}_\infty$ chains. The complex cations in compounds 1–3, 6, 8 and 15 were found to be disordered, which suggests only very weak (negligible) interactions between cations and anions so that these chains are straight. A noteworthy point is the number of the free en molecules that co-crystallized in compounds 10–14. The number of en molecules in type II compounds is 1 and in type III is 0.5, which are fixed for all the examples found displaying the same type. Although the relationship between the types and the number of en molecules is still unclear, it is doubtless that the different number of free en molecules have a significant effect onto the structural motifs of 1D $\{[InTe_2]^{n-}\}_\infty$ anionic chains via N—H···Te H-bonding interactions.

Another infinite 1D $[M_2Q_6]^{2-}$ chains constructed by the fused five membered rings of $[(M^{3+})_2(Q_2{}^{2-})(Q^{2-})]$ (M = In, Q = Te) joined at the M atoms, have been found in $[M(en)_3][In_2Te_6]$ (M = Fe(17), Zn(18)), α and β-$[Mo_3(en)_3(\mu_2\text{-}Te_2)_3\text{-}(\mu_3\text{-}Te)(\mu_3\text{-}O)][In_2Te_6]$(19) [16]. The similar Group 12–13/chalcogen five-membered ring has been also observed in 1D polymeric compounds like $(Ph_4P)_2[In_2Te_6]$ [74]. The repeating unit consists of four In_2Te_3 rings with a period of 16.27 Å for 17 and 18, 14.50 Å for 19α and 11.55 Å for 19β. The different length of repeating units among them reflects the high degree of flexibility of these $[In_2Te_6]^{2-}$ chains.

So far, only one report of a Group 13 chalcogenidoindate sheet anion has appeared in $[Zn(en)_3]_4[In_{16}(Te_2)_4(Te_3)Te_{22}]$(20) [17]. Four supertetrahedron In_4Te_{10} clusters (T_2; Fig. 15a) are held together to form a cyclic ring ($In_{16}Te_{35}$) by Te atoms (Fig. 15b). The unusual cyclic $In_{16}Te_{35}$ has a C_2 symmetry, with its 2-fold axis passing through the central Te1 atom. The supertetrahedron cluster can be described as tetrahedrally shaped fragments of the cubic ZnS-type lattice, which are recently denoted as T_n by Yaghi and co-workers [1c] where n is the number of metal layers. Although there are a series of similar T_2 supertetrahedron clusters $[M_{4-x}M'_xQ_{10}]^{8-x}$ (M = Ga, In; M′ = Ge, Sn; Q = S, Se) containing tri- or tetra-valent metals [1a], which are linked in T_d symmetry by the four terminal chalcogen atoms to extend into 3D open-frameworks, and the cations of these compounds are all protonated organic amines. Therefore, compound 20 is the rare example of a layer structure containing a supertetrahedron cluster with metal complexes as counterions.

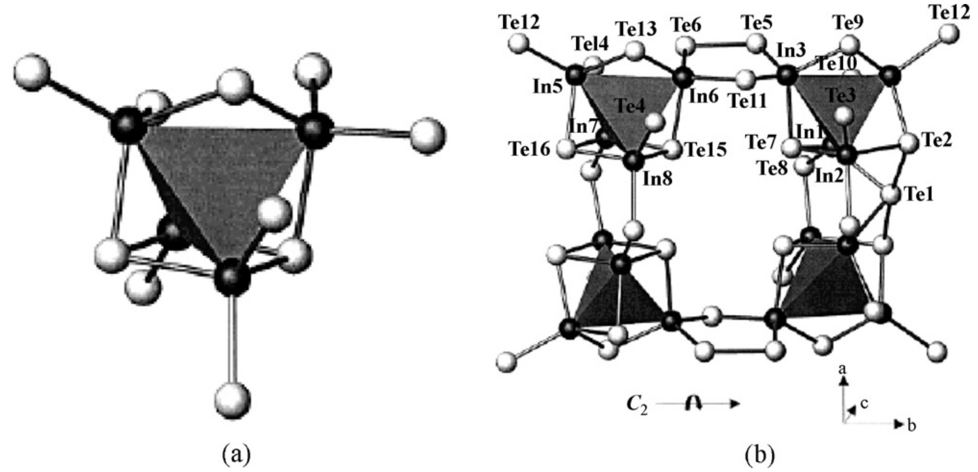

(a) (b)

Fig. 15. View of the In_4Te_{10} supertetrahedron (T_2) (a) and the $In_{16}Te_{35}$ fragment (b) found in $[Zn(en)_3]_4[In_{16}(Te_2)_4(Te_3)Te_{22}]$ with view approximately down the c axis [17].

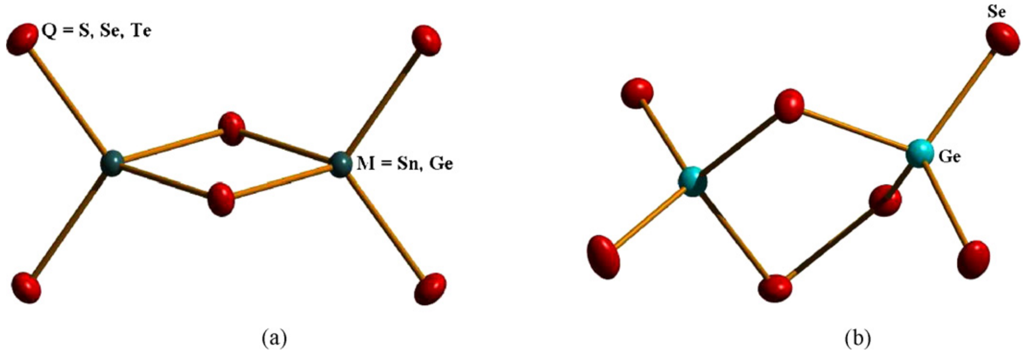

(a) (b)

Fig. 16. Dimeric anions (a) $[M_2Q_6]^{4-}$ in $[Mn(en)_3]_2[Sn_2Q_6]$ (Q = S(25)) [13f], Se(39) [20], Te(41) [21]) and $[Mn(en)_3]_2[Ge_2S_6]$(48) [13h] and (b) $[Ge_2Se_6]^{4-}$ in $[Mn(dien)_2]_2(Ge_2Se_7)$(53) [25].

3.1.2. Crystal structures of Group 14 chalcogenidometalate (Ge, Sn) anions

Two tetrahedral *ortho*-anions MQ_4^{4-} (M = Ge, Sn; Q = S, Se, Te) are easy condensed by edge-bridging to afford dimeric anions $[M_2Q_6]^{4-}$ (Fig. 16a). A series of hexachalcogenidometalates of the Group 14 elements with the general formula $A[M_2Q_6]$ (A = metal complex cation, Q = S, Se, Te) have been prepared by several groups with different methods in solution. The transition metal thiostannates $[Ni(en)_3]_2[Sn_2S_6]$(28) and $[Ni(dap)_3]_2[Sn_2S_6]\cdot 2H_2O$(30) were synthesized by Bensch et al. [11b] with M, Sn and S in en (or dap) at 140–200 °C. Similar conditions were employed by Guo and co-workers [18] to prepare the compounds $[Mn(en)_3]_2[Sn_2S_6]\cdot 2H_2O$(36) and $[Mn(dien)_2]_2Sn_2S_6$(37). Transition metal thiostannates $[M(en)_3]_2[Sn_2S_6]$ (M = Mn(25), Co(26), Zn(27), Ni(28)) [13f,g], $[Ni(dien)_2]_2[Sn_2S_6]$(29) [13g] and transition metal thio/selenidogermanates $[M(en)_3]_2[Ge_2S_6]$ (M = Mn(48), Ni(49)) [13h], $[Mn(en)_3]_2[Ge_2Se_6]$(50) [13m], and $[Fe(dien)_2]_2[Ge_2Se_6]$(51) [13m] were prepared by our group from metal chlorides or oxides in en or dien. Subsequently, our group successfully obtains six lanthanide chalcogenidostannates $[Ln_2(en)_6(\mu_2\text{-}OH)_2][Sn_2S_6]$(Ln = Dy(31), Er(32)), Nd(33), Gd(34)), $[Gd(dien)_3]_2[(Sn_2S_6)Cl_2]$(35) and $[Dy_2(en)_6(\mu_2\text{-}OH)_2][Sn_2Se_6]$(45) by the replacement of transition metal with lanthanide metal under similar mild solvothermal conditions [14a,b]. Chen and Wang [20] and Duan et al. [19] prepared transition metal selenidostannates $[M(en)_3]_2[Sn_2Se_6]$ (M = Ni(38), Mn(39), Zn(40)) by replacement of S with Se in the similar reaction. Analogous transition metal telluridostannates $[M(en)_3]_2[Sn_2Te_6]$ (M = Mn(41), Zn(42)) [21] are obtained from mixtures of $SnTe_2/MnCl_2/Te$ or $Cs_2Te/ZnCl_2/SnCl_2/Te$ in en at about 180 °C. In addition, milder solution technique was also applied for $[Mn(en)_3]_2[Sn_2Te_6]\cdot 4H_2O$(43) [22], which was achieved via the reaction of $Na_4(en)_4][SnTe_4]$ with $Mn(OAc)_2\cdot 4H_2O$ in water at room temperature. However, no report of the synthesis and the structural characterization of $[Ge_2Te_6]^{4-}$ anions with complex cations has appeared until now.

The cyclic $[Ge_2Se_7]^{4-}$ anion is formed by tetrahedral *ortho*-anions $[GeSe_4]^{4-}$ linked at one common Se atom and a Se–Se bond (Fig. 16b). The unique two examples of the formula type $A[Ge_2Se_7]$ (A = metal complex cation) are $(enH_2)[\{Mn(en)_2(enH)\}_2(\mu\text{-}en)](Ge_2Se_7)_2$(52) [25] and $[Mn(dien)_2]_2(Ge_2Se_7)$(53) [25]. The former was obtained by the reaction of Ge, Se and $Mn(OOCCH_3)_2\cdot 4H_2O$ in the presence of the mineralizer $[(CH_3)_2NH_2]Cl$ in a mixed solvent of en and CH_3OH at 150 °C, while the latter were prepared by a similar method, except that $[(CH_3)_2NH_2]Cl$ was replaced by Na_2CO_3 in en.

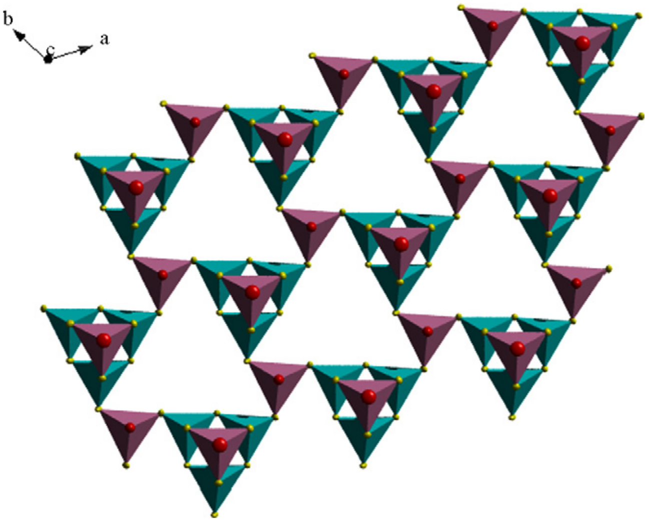

Fig. 18. View of the two-dimensional sheet in $[Ge_3S_6Zn(H_2O)S_3Zn(H_2O)][(Zn(tren)(H_2O))]$(54) [26].

Chen et al. attempted introducing chalcophilic transition metal ions ($CdCl_2$ or AgCl) into the $SnTe/Te/MnCl_2/en$ reaction system, two multimetallic tellurides $[Mn(en)_3][CdSnTe_4]$(46) and $[Mn(en)_3][Ag_6Sn_2Te_8]$(47) were successfully isolated [24]. The linear $[CdSnTe_4]^{2-}$ chain anion in 43 is formed by zig-zag "fused" $CdTe_4$ and $SnTe_4$ tetrahedra (Fig. 17a). The structure of 47 contains 2D double layers (Fig. 17b) of $[Ag_6Sn_2Te_8]^{2-}$ formed by connecting two single honeycomb-like layers through M—Te bonds (M = Ag, Sn).

It is important to note that the presence of in situ generated metal complexes easily tend to form the binary dimeric $[M_2Q_6]^{4-}$ or $[M_2Q_7]^{4-}$anion. But when chalcophilic transition metal ions are incorporated onto Group 14 chalcogenidometalate networks, the structural motifs of the anions become abundant. Although the synthetic procedures, the reactants and the solvent are essentially the same, compounds 46 and 47 are quite different in structure from that of 41. The results indicate that polymeric structure of chalcogenidometalate might be achieved only by adding chalcophilic transition metal ions (such as Cd(II) or Ag(I)).

As one more example, Feng and co-workers have recently reported a 2D thiogermanate $[Ge_3S_6Zn(H_2O)S_3Zn(H_2O)][(Zn(tren)(H_2O))(54)]$ [26] prepared by the reaction of GeO_2,

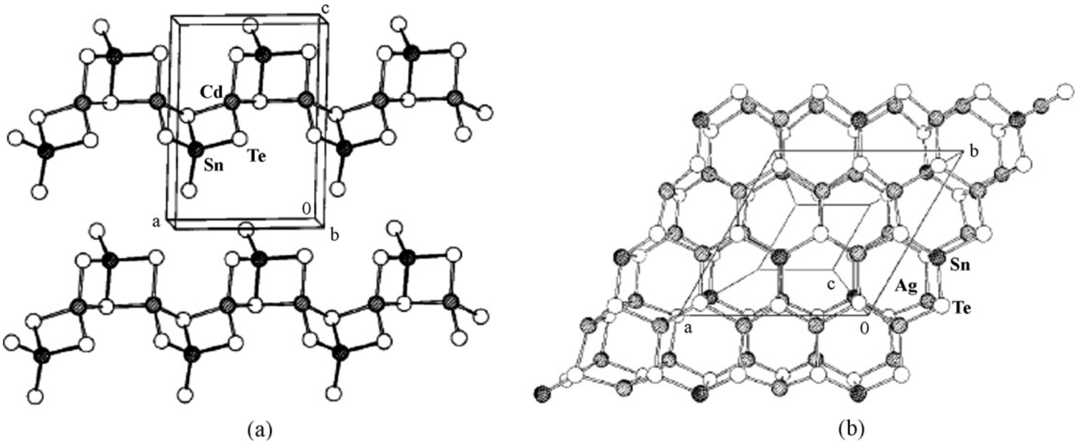

Fig. 17. (a)View along the *b* axis showing the $[(CdSnTe_4)^{2-}]_n$ 1D chains in $[Mn(en)_3][CdSnTe_4]$(46) [24]. (b)View of a $[Ag_6Sn_2Te_8]^{2-}$ honeycomb-like double layer in $[Mn(en)_3][Ag_6Sn_2Te_8]$(47) [24].

$Zn(NO_3)_2{\cdot}6H_2O$ and S in tris(2-aminoethyl)amine (tren) at 190 °C. Its structure consists of a layered framework with the composition $[Ge_3S_6Zn(H_2O)S_3Zn(H_2O)]^{2-}$ and a divalent charge-balancing complex cation $[Zn(tren)(H_2O)]^{2+}$. Within each infinite sheet (Fig. 18), three Ge and one Zn cation build a T_2 cluster. All Ge atoms are tetrahedrally coordinated by S atoms, but three S atoms are bound to Zn site and fourth corner of Zn^{2+} is occupied by one water molecule (Fig. 19a). Unlike most other chalcogenidometalates in which the four terminal chalcogen atoms are linked in T_d symmetry, both $[Ge_3S_9Zn(H_2O)]^{4-}$ T_2 clusters adopt a 3-connected mode forming a layered thiometalate framework, due to the corner termination by one water molecule on each zinc site. Each space in the ring encapsulates one complex (Fig. 19b) so that the negative charge from the sulfide sheet is balanced by the charge on the metal complex.

3.1.3. Crystal structures of Group 15 chalcogenidometalate (As, Sb) anions

Compounds of the formula type AMQ_4 (A = transition metal or lanthanide metal complex cation, M = Sb, Q = S, Se) (Fig. 20a) with

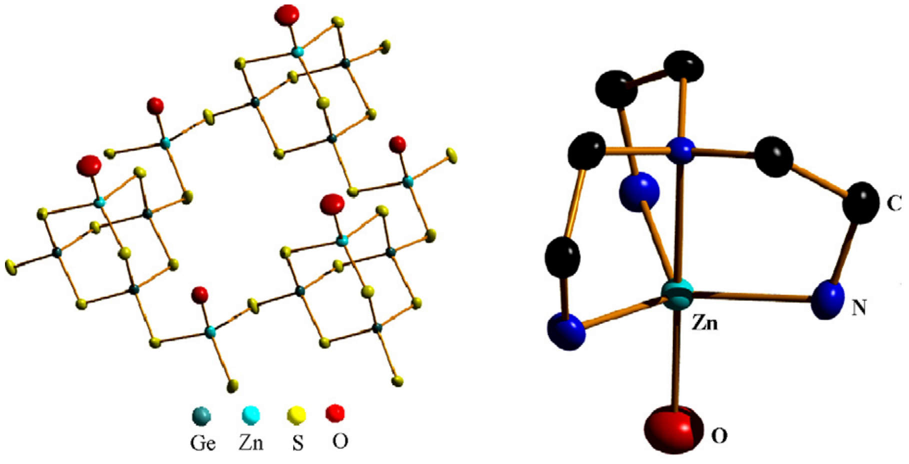

(a) (b)

Fig. 19. (a) The 9-member ring window made from alternating T_2 and T_1 clusters. (b) The structure of the structure directing molecule in 54 [26].

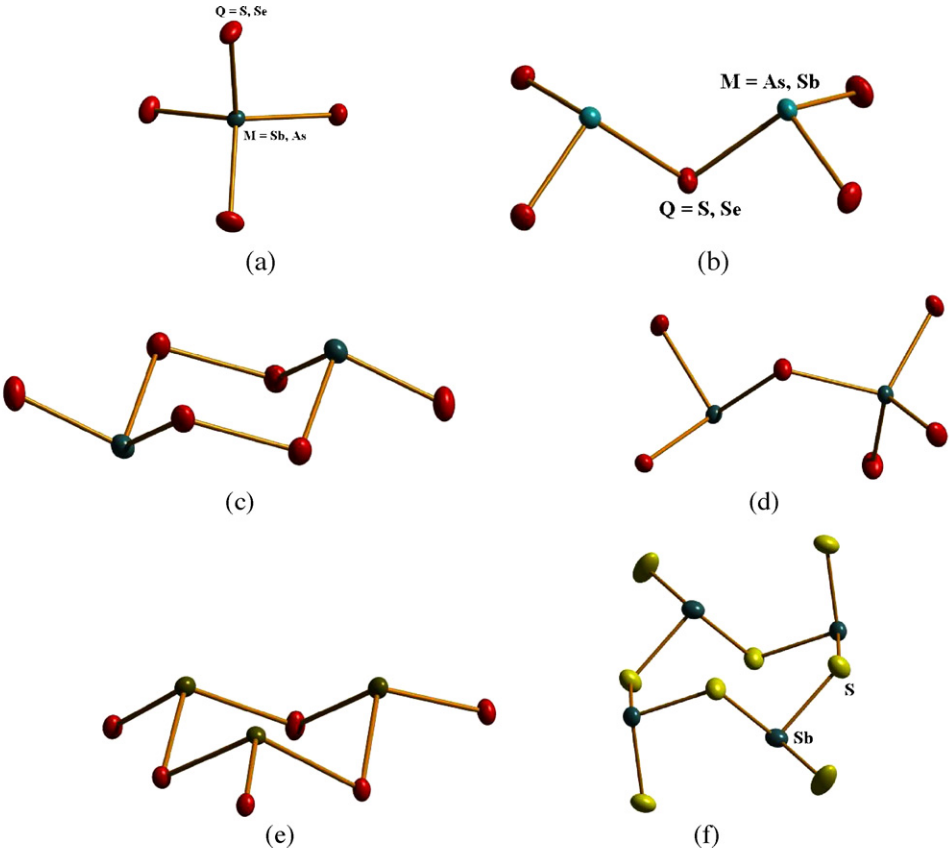

(a) (b) (c) (d) (e) (f)

Fig. 20. Chalcogenidoantimonate/arsenate anions: (a) $[MQ_4]^{3-}$ [10b,e,13j,14c–f,29–31], (b) $[M_2Q_5]^{4-}$ [13k,j,32–34], (c) $[As_2Se_6]^{2-}$ [36], (d) $[Sb_2Se_6]^{4-}$ [33], (e) $[As_3Se_6]^{3-}$ [36], (f) $[Sb_4S_8]^{4-}$ [10c].

the tetrahedral *ortho*-anions $[MQ_4]^{3-}$ have been structurally characterized. These compounds include thio/selenidoantimonates(V): $[Cr(en)_3][SbS_4]$(72) [10b], $[Ni(en)_3]_2(SbS_4)(NO_3)$(79) [29], $[Ni(dien)_3]_3(SbS_4)_2$(80) [30], $[Ni(en)_3(Hen)][SbS_4]$(78) [13j], $[M(en)_3(Hen)][SbSe_4]$ (M = Fe(81), Co(82), Ni(83), Mn(84)) [10e,31], and lanthanide metal thio/selenidoantimonates (V) $[Ln(en)_4][SbS_4]\cdot 0.5en$ (Ln = Eu(73), Dy(74), Yb(75), Sm(76), Gd(77)) [14c–e], $[Sm(en)_4][SbSe_4]\cdot 0.5en$(85) [14f]. The structures of compounds 78 and 81–84 contain both coordinated and protonated amines, due to the compensation of the negative charge of the $[SbS_4]^{3-}/[SbSe_4]^{3-}$ anion.

Corner-sharing $Sb^{III}S_3$ trigonal pyramids lead to dimeric saddle anions $[M_2Q_5]^{4-}$ (M = As, Sb; Q = S, Se), in which two SbS_3 trigonal pyramids are in *cis*-conformation (Fig. 20b). These examples have been found as $[M(en)_3]_2[As_2S_5]$ (M = Mn(92), Ni(93)) [13k], $[Mn(en)_3]_2[As_2Se_5]$(94) [13k], $[Fe(en)_3]_2[Sb_2S_5]\cdot 0.55H_2O$(86) [32], $[Mn(en)_3]_2[Sb_2S_5]$(87) [13j], $[Ni(dien)_2]_2[Sb_2Se_5]$(88) [33] and $[Fe(en)_3]_2[Sb_2Se_5]$(89) [34]. Corner-sharing a $Sb^{III}Se_3$ trigonal pyramid and a Sb^VSe_4 tetrahedron results in the dimeric $[Sb_2Se_6]^{4-}$ anion (Fig. 20d). The only example that has been found is $[Co(dien)_2]_2[Sb_2Se_6]$(99) [33] obtained by a reaction of $CoCl_2$, Sb and Se_4 in dien at 140 °C, which has been recently reported. The chalcogenidoantimonates (V) are seldom interconnected to form a poly-anion and always exist as an isolated tetrahedral $[Sb^VQ_4]^{3-}$ anion except that in some cases $[Sb^VQ_4]^{3-}$ is bound to metal complex cations [14c–e]. The mixed valent $[Sb_2Se_6]^{4-}$ anion in 99 contains Sb^{III} and Sb^V. Up to now the poly-anion containing similar mixed-valent Sb atoms have been only observed in $[Ni(dien)_2]_2[Sb_4S_9]$(117) [42] and $[M(dien)_2]_2[Sb_4Se_9]$ (M = Mn(118), Fe(119)) [33]. The structural features of these three compounds will be discussed latter.

Connection of pyramidal $AsSe_3$ units by two Se—Se bonds can afford dimeric anions $[As_2Se_6]$, which can be described as a six-membered As_2Se_4 ring with chair conformation (Fig. 20c). Fu et al. prepared $[M(en)_3][As_2Se_6]$ (M = Fe(96), Mn(97)) [36] with Fe (or Mn), As and Se in a mixed en–water solution at 180 °C. Vertex-linking of three $[MQ_3]^{3-}$ trigonal pyramids can lead to cyclic $[M_3Q_6]^{3-}$ (Fig. 20e). In $[Ni(dien)_2]_3[Sb_3S_6]_2$(100) [10a] and $[Mn(dien)_2]_3[As_3Se_6]_2$(98) [36], the six-membered M_3Q_6 rings display chair conformations with terminal chalcogen atoms in the equatorial position. The similar cyclic anions $[As_3S_6]^{3-}$ and $[As_3Se_6]^{3-}$ have been observed in $(enH_2)_3[As_3S_6]_2\cdot 6en$ [75] and $[Sr(en)_4]_2[AsSe_3]Cl$ [76] which were isolated from a reaction product of a synthesis in en solution. Four pyramidal SbS_3 units sharing common corners build a Sb_4S_4 hetero-ring (Fig. 20f) in $[Ni(dien)_2]_2[Sb_4S_8]$(103) [10c] prepared by the reaction of Ni, Sb

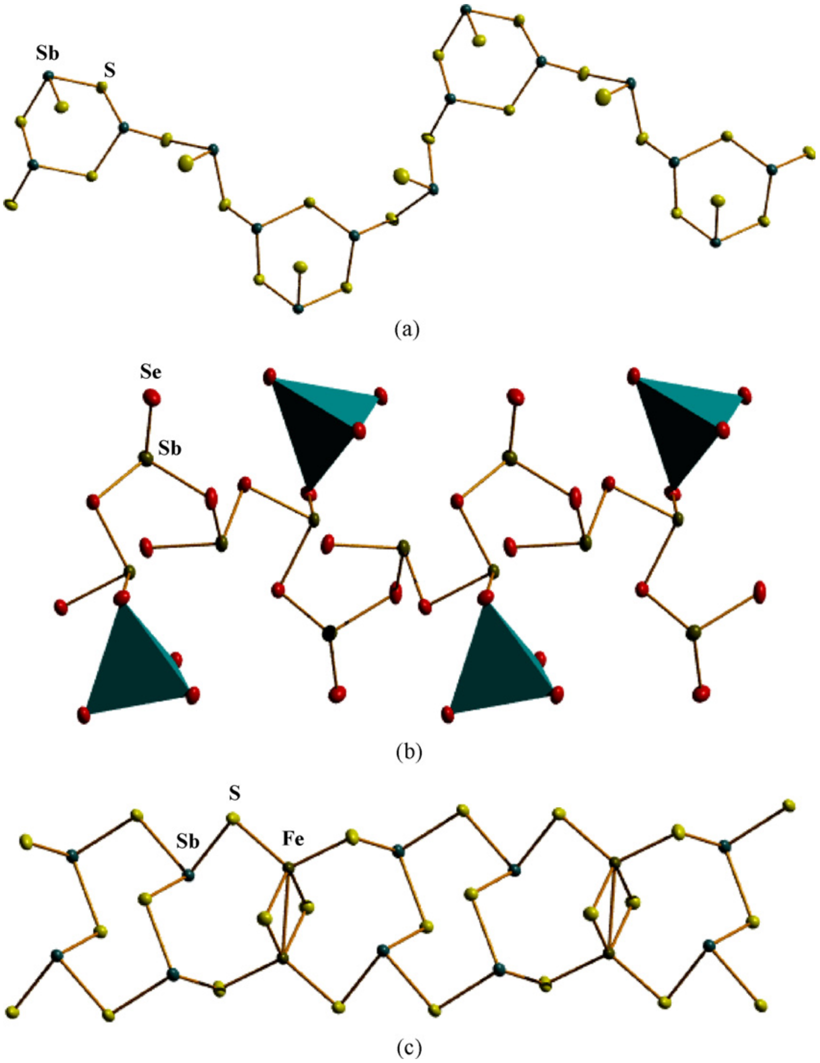

Fig. 21. Polymeric chain-like anions: (a) $[Sb_4S_7{}^{2-}]_\infty$ chains in $[M(en)_3][Sb_4S_7]$ (M = Co(105), Mn(106), Fe(107), Ni(108)) [37–39], (b) $[Sb_4Se_9{}^{4-}]_\infty$ chains in $[M(dien)_2]_2[Sb_4Se_9]$ [M = Mn(118), Fe(119)] [33] and (c) $[Fe_2Sb_4S_{10}{}^{2-}]_\infty$ chains in $[Fe(dien)_2][Fe_2Sb_4S_{10}]$(121) [43].

and S in dien at 145 °C. This ring adopts the bent flexible chair conformation.

Repeated corner-bridging of $[SbS_3]^{3-}$ trigonal pyramids leads to the formation of the infinite $[SbS_2^{-}]_\infty$ chains (Fig. 9a) that have been observed in $[M(en)_3][Sb_2S_4]$ (M = Co(101), Ni(102), Fe(104)) [32,37] all were prepared in en. Such polymeric anions are also found in $[Ba(en)_4][Sb_2Se_4]$ [77] prepared under solvothermal conditions, as well as $AAsSe_2$ (A = K, Rb, Cs) [78] isolated from a product of a methanothermal synthesis. Corner-bridging of $[SbS_3]^{3-}$ trigonal pyramids can also lead to the formation of a cyclic anion $[Sb_3S_6]^{3-}$ with six-membered rings in chair conformation, which are further linked by individual SbS_3 forming an infinite zigzag $[Sb_4S_7]^{2-}$ chain (Fig. 21a). This connectivity pattern is found in $[M(en)_3][Sb_4S_7]$ (M = Co(105), Mn(106), Fe(107), Ni(108)) [37–39]. Analogous $[M_4S_7]^{2-}$ chains have also been reported for $(Me_4N)_2[As_4S_7]$ [79], $[pipH_2][Sb_4S_7]$ [80] and $[NH_4]_2[Sb_4S_7]$ [81], in which the protonated amine, ammonium or tetra-alkylammonium ion acts as counterion. With the exception of $[SbQ_3]^{3-}$ trigonal pyramids as main building units, the $Sb^{V}Q_4$ [or MS_4 (M = transition metal)] tetrahedron as secondary building block leads to the assembly of a variety of structure types. The $[Sb_4Q_9{}^{4-}]_\infty$ anionic chains (Fig. 21b) in $[Ni(dien)_2]_2[Sb_4S_9]$(117) [42] and $[M(dien)_2]_2[Sb_4Se_9]$ [M = Mn(118), Fe(119)] [33] are constructed by Sb_3Q_6 and $Sb^{V}Q_4$ units. In $[Fe(dien)_2][Fe_2Sb_4S_{10}]$(121) [43], the $[Fe_2Sb_4S_{10}{}^{2-}]_\infty$ anionic double chain (Fig. 21c) is formed by the interconnection of two $[Sb_2S_5]$ units and one $[Fe_2S_6]$ unit.

The 2D porous $[Sb_4S_7{}^{2-}]_n$ layers in $[M(dap)_3][Sb_4S_7]$ (M = Ni(109), Co(110)) [13l] with the large ellipsoidal 32-membered $Sb_{16}S_{16}$ rings have been discussed above with respect to the structure directing role of complex cations (Fig. 5a). The apertures of the $Sb_{16}S_{16}$ hetero-rings are filled by two $[M(dap)_3]^{2+}$ complex cations which serve as template ions. However, for $[Ni(dien)_2][Sb_4S_7]\cdot H_2O$(111) [40a], a 2D layered anion, the *mer*-$[Ni(dien)_2]^{2+}$ cations are located above and below the layers leading to a sandwich-like arrangement. Different connectivities are also found for the pseudo-SbS_3 tetrahedra and pseudo-SbS_4 trigonal bipyramids in 2D thioantimony(III) compounds 109, 111 and $[Fe(dien)_2][Sb_6S_{10}]\cdot 0.5H_2O$(122) [44]. The ability of Sb(III) to extend its coordination number to 5 (in rare examples) in thioantimonates(III) leads to a fascinating diversity, and the only example that has been reported is $[Ni(dien)_2]_9[Sb_{22}S_{42}]\cdot 0.5H_2O$(125) [45]. Besides pseudo-$[SbS_3]^{3-}$ tetrahedra and pseudo-$[SbS_4]^{3-}$ trigonal bipyramids, pseudo-SbS_5 octahedra are observed.

Chalcogenidoantimonates/arsenates prepared by solvothermal methods commonly exhibit low-dimensional structures. So 3D chalcogenidoantimonates(III) with larger complex cations are very limit, so far only four examples were reported, i.e., $[Ni(cyclam)][Sb_4S_7]$(115) [41], $[Co(cyclam)]_x[cyclamH_2]_{1-x}[Sb_4S_7]$ $(0.08 \le x \le 0.74)$(116) [41], $[Co(en)_3][Sb_{12}S_{19}]$(123) [10d] and $[Ni(dien)_2]_3[Sb_{12}S_{21}]\cdot H_2O$(124) [45]. No 3D chalcogenidoarsenate has been reported until now. The condensation of the different pseudo-$[SbS_3]^{3-}$ tetrahedra and pseudo-$[SbS_4]^{3-}$ trigonal bipyramids as primary units yields Sb_xS_x rings (x = 2, 3, 4, 8, and 32). These complex cations act as a templating agent residing in the channel structure of the thioantimonate framework. Compounds 115 and 116 possess the same 3D $[Sb_4S_7]^{2-}$ framework, constructed from layers of parallel arrays of $[Sb_4S_8]^{4-}$ chains stacked at 90° to one another (Fig. 22). The 3D $[Sb_{12}S_{19}]^{2-}$ anionic structure contains 1D circular channel in 123.

In fact, the dimensionality of the thioantimonate (III) network could often be somewhat arbitary in view of the Sb–S separations spread from about 2.3 Å up to the sum of the van der Waals radii of about 3.8 Å. In many cases Sb(III) has further S atoms at longer distances and if such Sb–S separations are treated as a secondary Sb–S interaction the dimensionality changes. For instance, in $[Ni(en)_3]Sb_4S_7$ [37], The Sb atoms have significant secondary Sb-S bonds (the distances vary from 3.066 to 3.560 Å), the infinite zigzag $[Sb_4S_7]^{2-}$ chains are connected via these secondary bonds to create a pseudo 2D network. In $[Ni(dap)_3][Sb_4S_7]$[13l], the 2D $[Sb_4S_7]^{2-}$ puckered layers interact also *via* similar secondary bonds forming a pseudo 3D network. Therefore, the assignment of the dimensionality should be treated with caution. The dimensionality of the thioantimonate (III) network in this review depends on the cut-off of less than ca. 3.0 Å for the Sb–S distances.

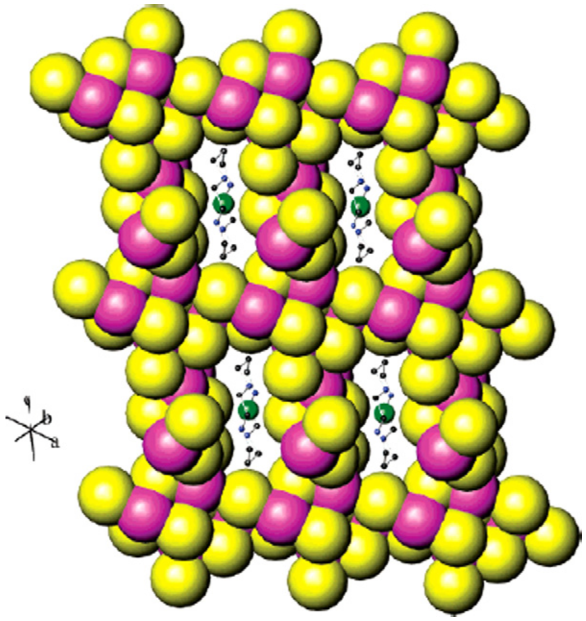

Fig. 22. Space-filling representation of the $[Sb_4S_7]^{2-}$ framework of $[Ni(cyclam)][Sb_4S_7]$ illustrating one set of channels and showing the location of the Ni^{2+}-chelate complex [41].

3.2. *Chalcogenidometalates with covalently linked metal complex cations*

These are ternary chalcogenidometalates $[A(amine)_nM_yQ_z]$ or $[A(amine)_nA_xM_yQ_z]$ of the heavier Group 13–15 elements (A = divalent transition metal or lanthanide metal ion; Group 13, M = Ga, In; Group 14, M = Ge, Sn; Group 15, M = As, Sb) with covalently linked complex cations and anions. The anionic framework of the Group 13–14 elements is constructed by tetrahedral *ortho*-anions $MQ_4{}^{4-}$ (M = Ga, In, Ge, Sn; Q = S, Se, Te), including dimeric anions $[Sn_2Q_6]^{4-}$ (Q = S, Se) [13d and e], 1D $[GaS_2]^-$ [11a], 1D $[In_4S_9H_2]^{4-}$ [13a], or the 1D $[Sn_3Se_7]^{2-}$ [13e] chain, and the $[Ga_4S_6(SH)_4]^{4-}$ [13c] supertetrahedral cluster. The Group 15 chalcogenidometalate anionic structures range from isolated $[MQ_4]^{3-}$ (M = As, Sb; Q = S, Se) tetrahedron or $[SbS_3]^{3-}$ [10b] trigonal pyramid to $[Sb_2S_5]^{4-}$ [54,55] dimeric anion, 1D $[Sb_2S_4]^{2-}$ or $[Sb_4S_7]^{2-}$ chain [50,61], and 2D $[Sb_2S_4]^{2-}$ [51] layered systems. Some transition-metal ions have been fully incorporated into the main group framework to form heterobimetallic anions, such as the trimeric $[Mn(SnTe_4)_2]^{6-}$ anion [12], the 1D $[FeSbS_4]^{2-}$ chain [43], and the 1D $[Mn_2Sb_4S_{10}]^{4-}$ chain [54]. These chalcogenidometalate anions as ligands connect metal complex cations, forming a variety of structures.

3.2.1. *Crystal structures of Group 13 chalcogenidometalates (Ga, In)*

The binary anions in the compounds $\{[Mn(en)_2](Ga_2S_4)\}$(21) [11a] and $\{[Mn(atep)](Ga_2S_4)\}$(23) [13c] represent 1D $[GaS_2]^-$

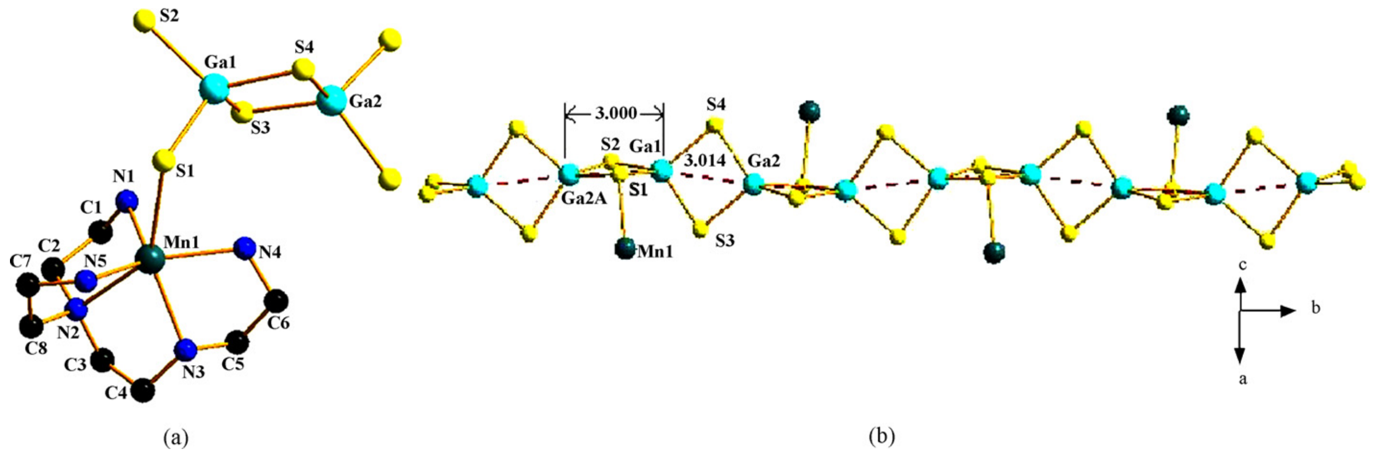

Fig. 23. (a) The structure of $\{[Mn(atep)](Ga_2S_4)\}$(23) [13c]. (b) View of the 1D chain showing the type II structure. All H, C and N atoms have been omitted for clarity.

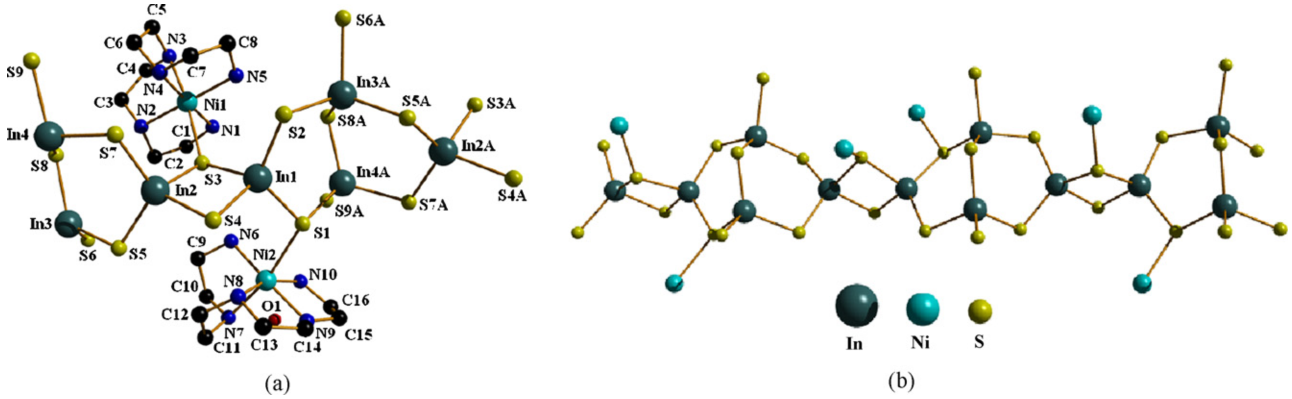

Fig. 24. (a) The structure of $[Ni(tepa)]_2[In_4S_7(SH)_2]\cdot H_2O$(24) [13a]. (b) The 1D chain of the polymeric anion in 24 (complex cations are omitted for clarity).

chains. The 1D polymeric structure of 23 consists of unusually sinusoidal $[Ga_4S_8{}^{4-}]_n$ anions (Fig. 23). The $[Mn(atep)]^{2+}$ complex cations are regularly bound to both sides of the chain *via* bridging S atoms of the anion (Fig. 23b). If complex cation leaves at least two coordination sites for bonding of S atoms of the anion, low dimensional chains could be extended into 2D layer or 3D network. The structure of 21 is closely related to this example and one-dimensional $[GaS_2]^-$ chains are linked into a 3D structure by unsaturated $[Mn(en)_2]^{2+}$ complex nodes (Fig. 12). A novel $[In_4S_9H_2]^{4-}$ chain built from InS_4 tetrahedra sharing corners and edges has been observed in $[Ni(tepa)]_2[In_4S_7(SH)_2]\cdot H_2O$(24) [13a]. In the polymeric anion of 24, four InS_4 tetrahedra are interconnected to an arachno-shaped In_4S_{11} clusters. The clusters are further linked via the edge-sharing forming an infinite chain $\{[In_4S_9]^{4-}\}_n$ (Fig. 24). The $[Ni(tepa)]^{2+}$ complex cations are regularly bound to the chain by In–S–Ni bridges. The singly coordinated S atoms (S6 and S9) have a bond to one H atom to form a terminal –SH group, which also been reported for other thioindates, such as $[(C_3H_7)_2NH_2]_3In_6S_{11}H$ [6e] and $[In_8S_{13}(S_3)_{1/2}(SH)][In_4S_6(S_3)_{1/2}(SH)](TMDPH_2)_5$ [82]. With the exception of 1D $[GaS_2]^-$ and $[In_4S_9H_2]^{4-}$ chains, supertetrahedral cluster $[Ga_4S_6(SH)_4]^{4-}$ anion as ligand bonds to the unsaturated $[Ni(tepa)]^{2+}$ ion by the bridging S atom, which has also been found in $\{[Ni(tepa)]_2SO_4\}[Ni(tepa)(Ga_4S_6(SH)_4)]$(22) [13c] (Fig. 25). A longer terminal In—S bond suggests that these S atoms are actually –SH groups, considering also the charge balance requirements of $[Ga_4S_6(SH)_4]^{4-}$.

3.2.2. *Crystal structures of Group 14 chalcogenidometalates (Ge, Sn)*

Tetrahedral *ortho*-anions $[MQ_4]^{4-}$ (M = Sn, Ge, Q = S, Se) as chelating or chelating/bridging ligands are seen in $[K_6(MeOH)_9][Sn_2Se_6][Cr(en)_2(SnSe_4)]_2$, $[Na(H_2O)_4][Cr(en)_3]_2[GeS_3OH]_2[Cr(en)_2(GeS_4)]$ and $[Ba(H_2O)_{10}][\{Cr(en)\}_2(GeSe_4)_2]$, [28] these

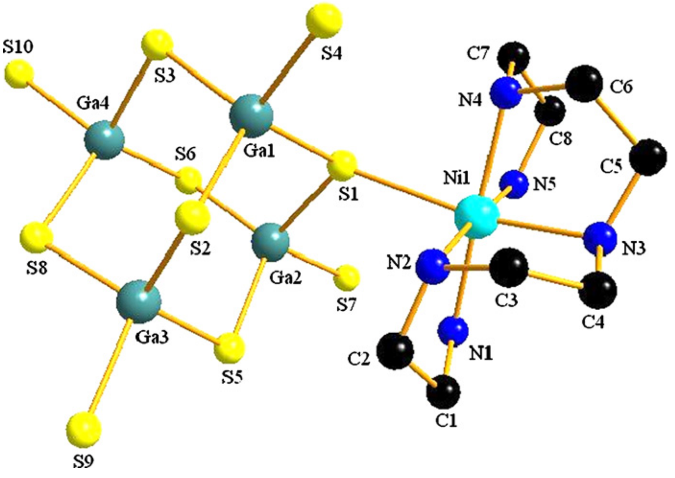

Fig. 25. The structure of $[Ni(tepa)(Ga_4S_6(SH)_4)]^{2-}$ anion in $\{[Ni(tepa)]_2SO_4\}[Ni(tepa)(Ga_4S_6(SH)_4)]$(22) [13c].

compounds have been prepared by a chemical route in solution under ambient conditions. Their structural motifs have been discussed by Dehnen and Melullis in a review article [2d]. The $[MQ_4]^{4-}$ anions exhibit a characteristic tendency to condense by corner- or edge-bridging to afford oligomeric entities or 1D chains under mild solvatothermal conditions. The dimeric $[Sn_2Q_6]^{4-}$ (Q = S, Se) anions display the different coordination modes in these chalcogenidostannates. Three coordination modes of the $[Sn_2Q_6]^{4-}$ anions have been observed. The first is that the $[Sn_2Q_6]^{4-}$ anions acts as bridging ligand by binding to two amine coordinated transition metal centers *via* a chalcogen atom. Fig. 6 shows the molecular structure of the dimeric $[Sn_2Se_6]^{4-}$ anion with covalently linked complex cation, considering compound 59 as example. The $[Sn_2Se_6]^{4-}$ anion connects two $[Mn(tepa)]^{2+}$ units by the trans terminal Se atoms forming the neutral $[Mn(tepa)]_2(\mu_2\text{-}Sn_2Se_6)$ compound with a center of inversion. Isotypic examples occurs in $[M(tepa)]_2(\mu_2\text{-}Sn_2Q_6)$ (Q = S, M = Mn; Q = Se, M = Fe, Co, Mn)[13d–e] and $[Co(tren)]_2(\mu_2\text{-}Sn_2S_6)$(55) [11b]. In contrast to $[Co(tren)]_2(\mu_2\text{-}Sn_2S_6)$ where Co^{2+} is only five-fold coordinated, the Ni^{2+} ion in $[Ni(tren)]_2(\mu_2\text{-}Sn_2S_6)$(56) [11b] is in a six-fold environment of one tetradentate tren ligand and two S atoms of two symmetry related $[Sn_2S_6]^{4-}$

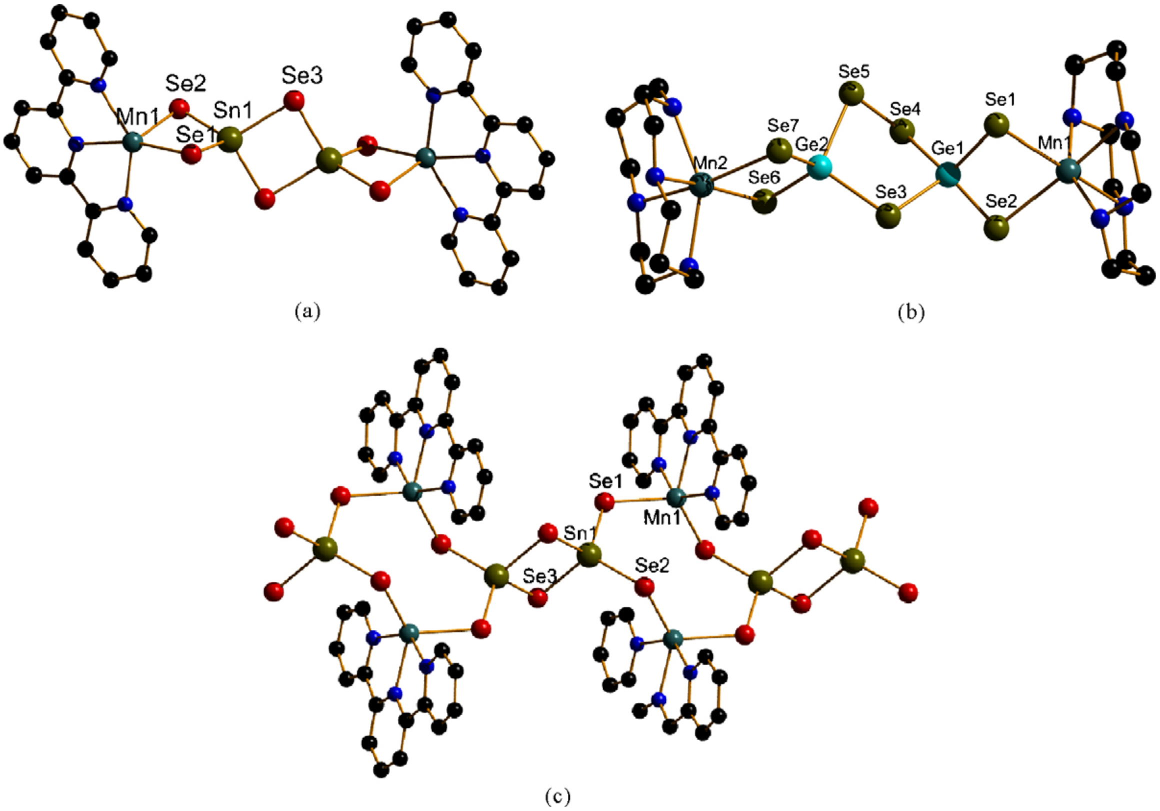

Fig. 26. (a) Molecular structure of [{Mn(terpy)}$_2$(μ-Sn$_2$Se$_6$)](62) [27b], (b) molecular structure of [{Mn(cyclam)}$_2$(μ-Ge$_2$Se$_7$)]·CH$_3$OH·1.5H$_2$O(64) [27b] and (c) a section of the infinite chain of [{Mn(terpy)}$_2$(μ-Sn$_2$Se$_6$)]$_n$(63) [27b].

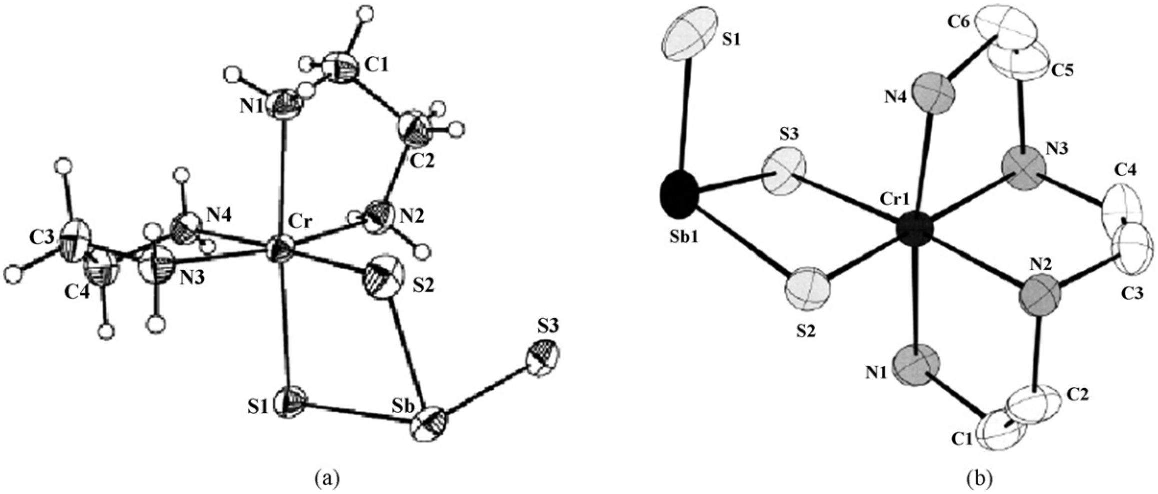

Fig. 27. Molecular structures of [Cr(en)$_2$SbS$_3$](126) [10b] (a) and [Cr(teta)SbS$_3$](127) [46] (b).

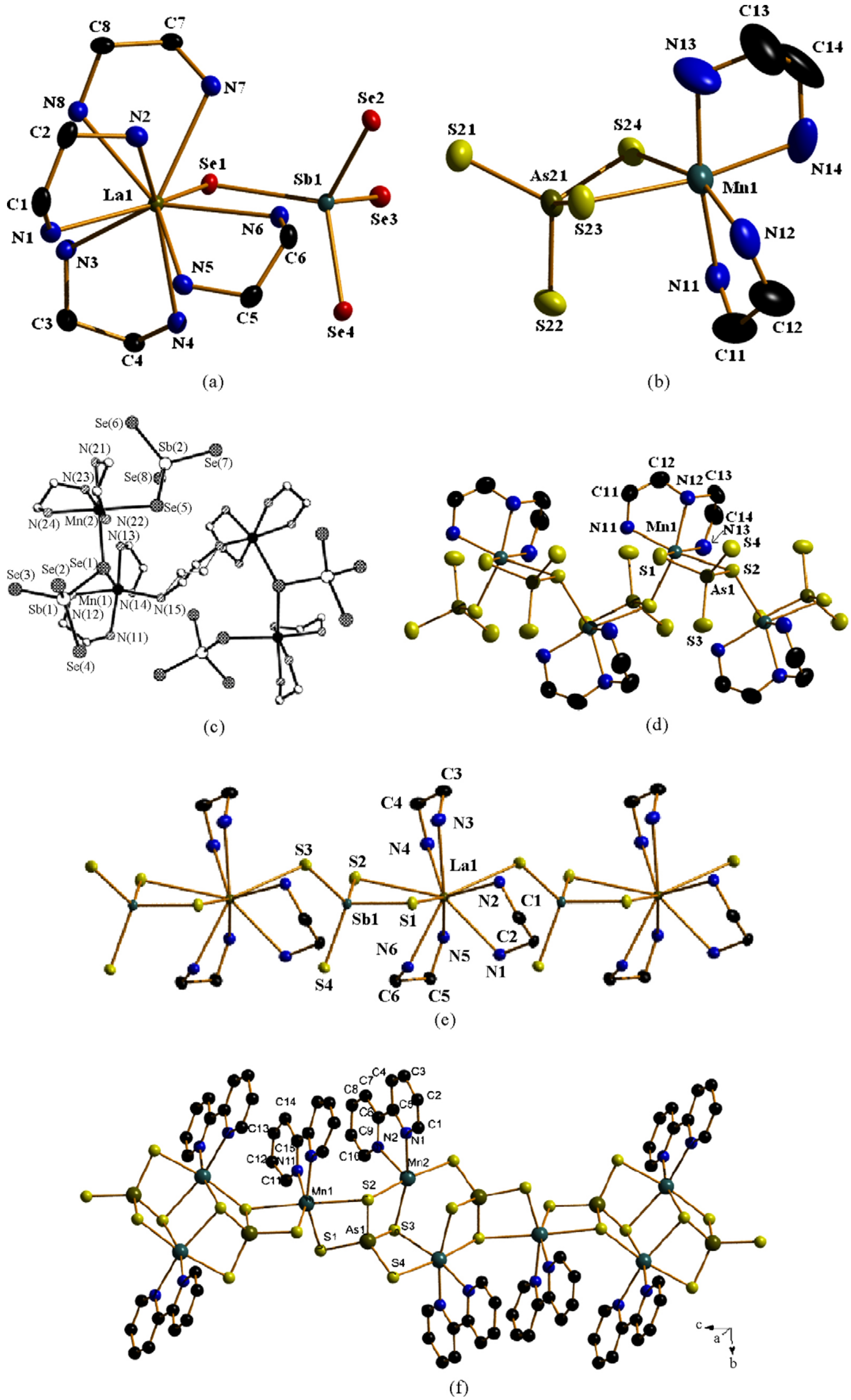

Fig. 28. (a) the mono-dentate mode in $[La(en)_4(SbSe_4)](137)$ [14f] (type I), (b) the bi-chelating mode in $[Mn(en)_3]_2[Mn(en)_2AsS_4][As_3S_6](170)$ [63a] (type II), (c) the mono-dentate bridging mode in $[Mn(en)_3]_2[Mn_4(en)_9(SbSe_4)_4]\cdot 2H_2O(136)$ [49] (type III), (d) the bi-dentate chelating/bridging mode in $[Mn(dien)_2]_n[Mn(dien)AsS_4]_{2n}\cdot 4nH_2O(169)$ [63a] (type IV), (e) the tri-dentate chelating/bridging mode in $[La(en)_3(\mu_3\text{-}SbS_4)]_n(128)$ [14c] (type V), (f) the tetra-dentate chelating/bridging mode in $[Mn_3(2,2'\text{-}bipy)_3(As^VS_4)_2]n\cdot nH_2O(171)$ [63b] (type VII).

anions. This connection mode leads to the formation of “zig-zag-like” Ni-Sn_2S_6 chains. The second is that the $[Sn_2Se_6]^{4-}$ anions exhibit a tetradentate chelating/bridging coordination mode to result in neutral centrosymmetric $[\{Mn(terpy)\}_2(\mu\text{-}Sn_2Se_6)]$(62) [27b] moieties (Fig. 26a). Examples for such mode analogues (Fig. 26b) are also observed in $[\{Mn(cyclam)\}_2(\mu\text{-}Sn_2Se_{6.15})]$(65) and $[\{Mn(cyclam)\}_2(\mu\text{-}Ge_2Se_7)]\cdot CH_3OH\cdot 1.5H_2O$(64) [27b]. The third is that the tetradentate $[Sn_2Se_6]^{4-}$ building units (Fig. 26c) bridge four $\{(terpy)Mn\}^{2+}$ fragments in the infinite chains of $[\{Mn(terpy)\}_2(\mu\text{-}Sn_2Se_6)]_n$(63) [27b]. Besides bridging ligand, a bridging coordination of en is observed in $[\{Mn(en)_2\}_2(\mu\text{-}en)(\mu\text{-}Sn_2S_6)]_n$(67) [13i]. Fig. 11 shows the 1D structure of 67 in a polyhedron model. The octahedral coordinated Mn(II) ions are alternately connected to the neighboring Mn(II) ions by an en and a $[Sn_2S_6]^{4-}$ bridge. So far, the only reported 1D thiostannate consisting of organic components is an unusual polymer $[SnS_2\cdot en]$ [83]. To the Sn(IV) center, an additional en ligand is chelated.

The structure of the 1D chiral compound $[Mn(tepa)\cdot Sn_3Se_7]_n$(66) [13e] (see Fig. 7b) is constructed by condensed Sn_3Se_4 cluster and a covalently bonded [Mn(tepa)] unit. It is notable that the flexible achiral tepa coordinates to Mn^{2+} ions, leading to a chiral center. The anion connected to the chiral metal complex cations by the terminal Se atoms. The infinite chiral chains are arranged in a parallel manner with the same orientation. Though the metal complex cations in 59 (or 60) are also chiral, the neutral $[Mn(tepa)]_2(\mu_2\text{-}Sn_2Q_6)$ molecule possesses a symmetry center, leading to an achiral configuration. Compounds

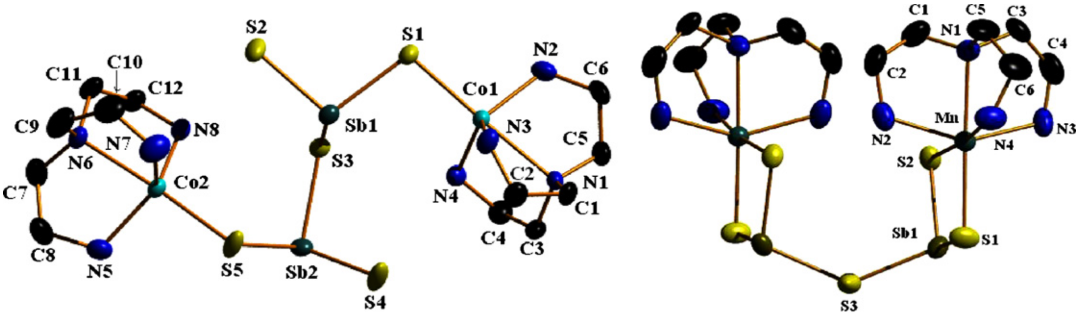

(a) (b)

Fig. 29. The molecular structures of $\{[Co(tren)]_2(Sb_2S_5)\}$(148) [55] (a) and $\{[Mn(tren)]_2(Sb_2S_5)\}$(147) [54] (b).

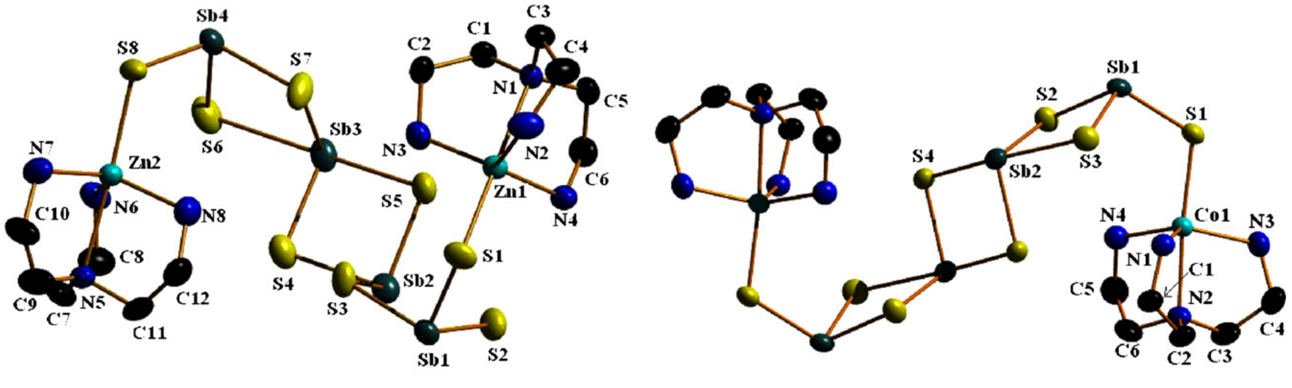

(a) (b)

Fig. 30. The molecular structures of $\{[Zn(tren)]_2(Sb_4S_8)\}\cdot 0.75H_2O$(156) [60] (a) and $\{[Co(tren)]_2(Sb_4S_8)\}$(157) [55] (b).

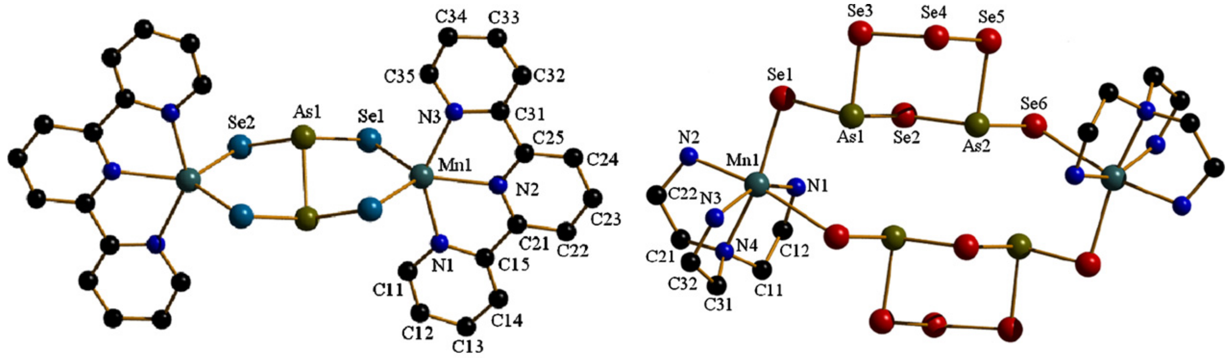

(a) (b)

Fig. 31. The molecular structures of $[\{Mn(terpy)\}_2(\mu\text{-}As_2Se_4)]\cdot 2H_2O$(146) (a) and $[\{Mn(tren)\}_2(\mu\text{-}As_2Se_6)_2]$(155) (b) [53].

66 and 59 were obtained under identical synthetic conditions and starting materials, but differed in the reaction time. An important feature of solvothermal syntheses is that metastable compounds are formed and the compounds isolated at the end of a synthesis may be the most stable one, but there are only very few examples of such phenomenon. In this case, compound 59 is the metastable product which is then transformed into the next stable 66 after prolonging the reaction time [13e].

Another type of 1D chiral chain has been observed in $[Mn(teta)(en)]\cdot[Mn(teta)][Mn(SnTe_4)_2\cdot Mn(teta)]$(71) [12], as shown in Fig. 8. The $[Mn3(teta)]^{2+}$ cation serves as the two-connected link to join the anion $[SnTe_4MnSnTe_4]^{6-}$ into a chiral

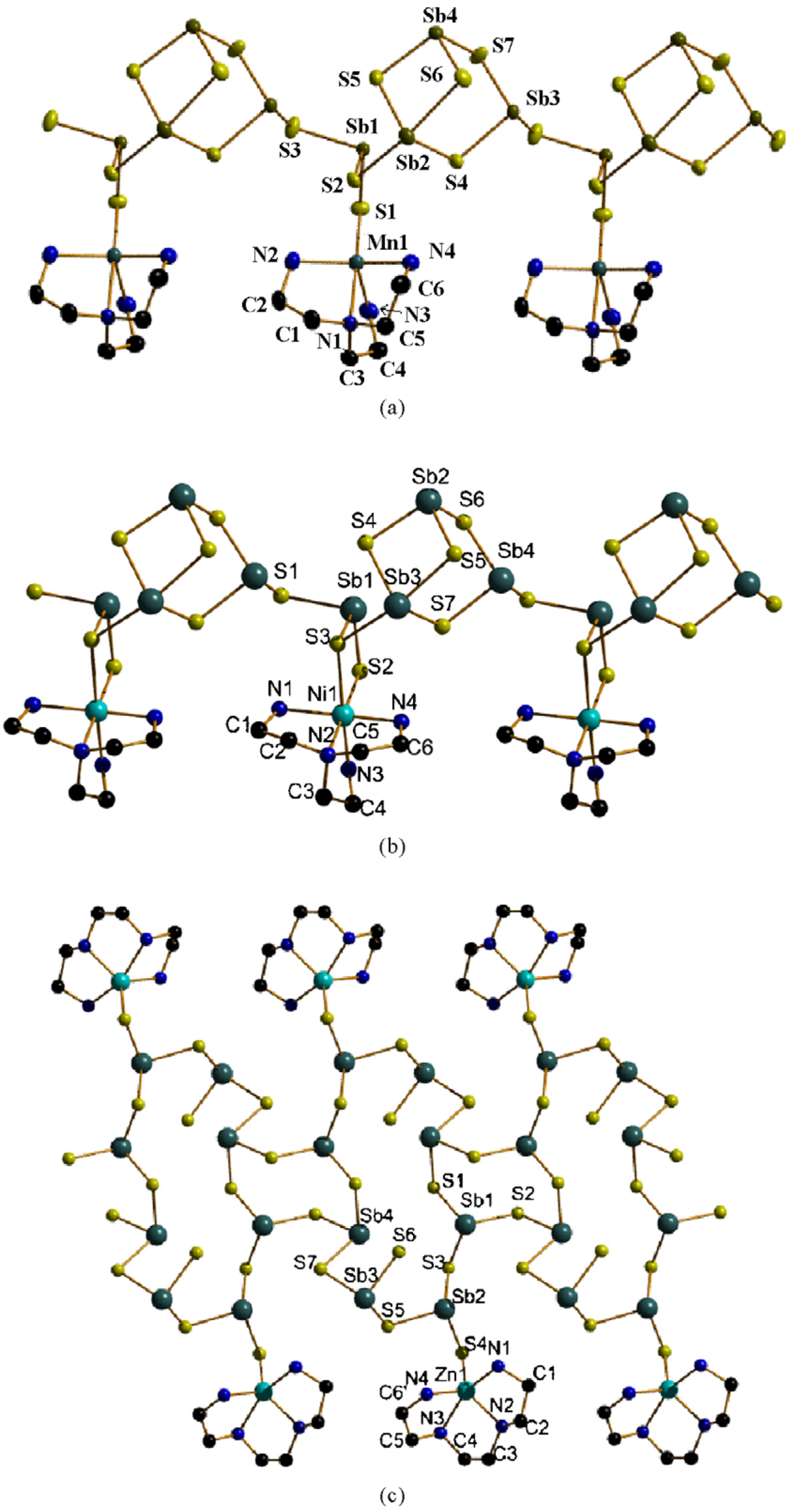

Fig. 32. The crystal structures of $\{[Mn(tren)](Sb_4S_7)\}$(158) [61] (a), $\{[Ni(tren)](Sb_4S_7)\}$(162) [40b] (b) and $\{[Zn(teta)](Sb_4S_7)\}$(164) [40b] (c).

helical chain. The $[Mn_2(teta)]^{2+}$ cations are connected by the terminal Te6 atom of the anion, regularly appended to both sides of the chain. The $[Mn4(teta)(en)]^{2+}$ complex serves to balance the negative charge on the anion and also contributes to the stabilization of the configuration of the helix. All helices are of the same chirality and are packed in a parallel manner, leading to a homochiral crystal.

3.2.3. *Crystal structures of Group 15 chalcogenidometalates (As, Sb)*

Though many alkali metal (or alkaline earth metal) chalcogenidometalates of Goup 15 elements with discrete pyramidal $[MQ_3]^{3-}$ anions (M = As, Sb; Q = S, Se) [84] are known, the examples with the $[MQ_3]^{3-}$ anion acting as ligands are rare, and only two examples were reported, i.e., $[Cr(en)_2SbS_3]$(126) [10b] and $[Cr(teta)SbS_3]$(127) [46]. In 126, chromium is chelated by two ethylendiamine molecules and one bi-chelating SbS_3 group in a distorted octahedral coordination (Fig. 27a), while the Cr^{3+} ion in $[Cr(teta)SbS_3]$ is six-coordinated by two S atoms of the chelating SbS_3 group, and one chelating teta ligand (Fig. 27b). In contrast, the tetrahedral *ortho*-anions $[MQ_4]^{3-}$ (M = As, Sb; Q = S, Se) exhibit richer binding modes and six different binding modes have been discovered to date. Figs. 10 and 28 show the coordination modes of the $[MQ_4]^{3-}$ anion. For example, in $[La(en)_4(SbSe_4)]$(137) [14f], the coordination sphere around La^{3+} ion is completed by the Se1 atom of the monodentate $[SbSe_4]^{3-}$ anion (type I; Fig. 28a). Examples for type I analogues have been found in thioantimonates $\{[Mn(tren)(Htren)](SbS_4)\}$(132) [47], and $[Mn(chxn)_3]_2[Mn(chxn)_2(SbS_4)_2]\cdot 6H_2O$(133) [47]. Besides the monodentate $[SbSe_4]^{3-}$ anion, it also act as monodentate bridging mode (type III; Fig. 28c). In $[Mn(en)_3]_2[Mn_4(en)_9(SbSe_4)_4]\cdot 2H_2O$(136) [49], the $[Mn_4(en)_9(SbSe_4)_4]^{4-}$ anion is built up from two $SbSe_4$–$Mn(en)_2$–$SbSe_4$–$Mn(en)_2$ subunits, connected by a bridging en ligand, with the $[SbSe_4]^{3-}$ anions display I and III binding modes (Fig. 28c). Type II is similar to the mode of the aforementioned $[SbS_3]^{3-}$ anion (Fig. 28b). The only example is the thioarsenate compound $[Mn(en)_3]_2[Mn(en)_2AsS_4][As_3S_6]$(170) [63a], in which the Mn1 atom in the *cis*-$[Mn(en)_2AsS_4]^-$ anion is six-coordinated by two S atoms from a chelating $[AsS_4]$ group and two chelating en ligands. Type IV is closely related to the type III mode. The $[AsS_4]^{3-}$ anion adopts the bidentate chelating/bridging mode, which has been encountered in $[Mn(dien)_2]_n[Mn(dien)AsS_4]_{2n}\cdot 4nH_2O$(169) [63a] (Fig. 28d). The zigzag anionic chain, $[Mn(dien)(AsS_4)]_n{}^{n-}$, is composed of [Mn(dien)] fragments bridged by $[AsS_4]$ group. Each Mn atom is chelated by one tridentate dien ligand and coordinated by three S atoms from two $[AsS_4]$ groups to form a distorted octahedron with a *cis*-configuration. Type V is the tri-dentate chelating/bridging mode observed in $[La(en)_3(\mu_3\text{-}SbS_4)]_n$(128) [14c] (Fig. 28e). The $SbS_4{}^{3-}$ anion acts as a μ_3-SbS_4 bridging ligand with S1 and S2 coordinating to one $[La(en)_3]^{3+}$ ion and S3 coordinating to another $[La(en)_3]^{3+}$ ion to link the $[La(en)_3]^{3+}$ ions into a 1D coordination polymer $[La(en)_3(\mu_3\text{-}SbS_4)]_n$. The structure of another 1D chain polymer $[Nd(en)_3(H_2O)(SbS_4)]_n$(129) [14c] is closely related to that of $[La(en)_3(\mu_3\text{-}SbS_4)]_n$. The $[SbS_4]^{3-}$ anion acts as bidentate bridging ligand (type VI; Fig. 10) other than a tridentate one in 128, because the nine-coordinate environment of $[Nd(en)_3]^{3+}$ ion is satisfied by the coordination of one H_2O molecule. The $[SbS_4]^{3-}$ anion connects neighboring $[Nd(en)_3(H_2O)]^{3+}$ cations to form 1D polymer of 129. More complex type VII (Fig. 28f) is the tetra-dentate chelating/bridging mode in $[Mn_3(2,2'\text{-}bipy)_3(As^VS_4)_2]n\cdot nH_2O$(171) [63b]. $[Mn(2,2'\text{-}bipy)]^{2+}$ fragments were bridged by $[As^VS_4]$ groups to form 1D $[Mn_3(2,2'\text{-}bipy)_3(As^VS_4)_2]_n$ neutral chains, whereas the $[As^VS_4]$ tetrahedra multi-edge-share with Mn octahedra.

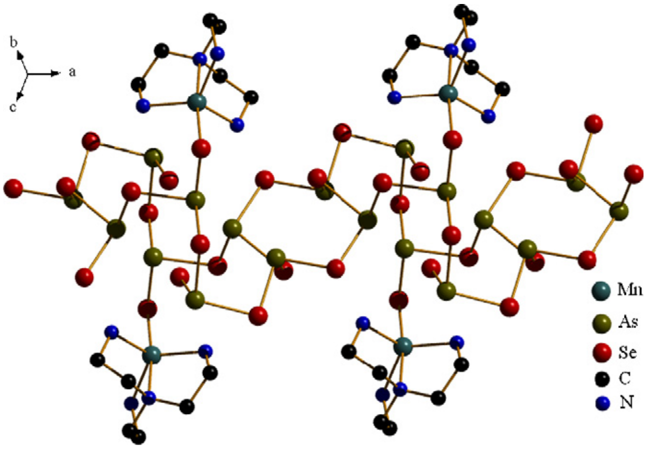

Fig. 33. A segment of the infinite double chains of $[\{Mn(tren)\}(As_4Se_7)]$(163) [52].

The $[Sb_2S_5]^{4-}$ anion displays two different types of coordination modes. In $\{[Co(tren)]_2(Sb_2S_5)\}$(148) [55], two terminal S atoms of the $[Sb_2S_5]^{4-}$ anion bridge two $[Co(tren)]^{2+}$ cation in a bidentate manner (Fig. 29a). The two SbS_3 trigonal pyramids are in *trans*-conformation, but discrete $[Sb_2S_5]^{4-}$ anion usually adopts *cis*-conformation [13j]. While the anion in $\{[Mn(tren)]_2(Sb_2S_5)\}$(147) [54] adopts the tetradentate chelating/bridging mode (Fig. 29b). Other bridging analogues have recently been reported by Bensch et al. $\{[Zn(tren)]_2(Sb_4S_8)\}\cdot 0.75H_2O$(156) [60] (Fig. 30a) and $\{[Co(tren)]_2(Sb_4S_8)\}$(157) [55] (Fig. 30b). In $[\{Mn(terpy)\}_2(\mu\text{-}As_2Se_4)]\cdot 2H_2O$(146) [53], two $[AsSe_2]$ units are connected by an As–As bond to form a tetradentate $[As_2Se_4]^{4-}$ ligand, adopting a staggered *trans*-conformation (Fig. 31a). $[\{Mn(tren)\}_2(\mu\text{-}As_2Se_6)_2]$(155) [53] contains two bridging bidentate $[As_2Se_6]^{2-}$ ligands, in which the As_2Se_4 ring can be regarded as being derived from the $[As_2Se_5]^{4-}$ anion by formation of two Se—Se bonds to an additional Se atom (Fig. 31b). Interestingly, no short S–S and Sb–Sb contacts are found in the aforementioned thioantimonates.

Condensation of SbS_3 and SbS_4 species by corner- or edge-bridging in the presence of suitable in situ generated metal complex cations can lead to different 1D or 2D poly-anionic ligands. Fig. 32a shows the crystal structure of the 1D chain in $\{[Mn(tren)](Sb_4S_7)\}$(158) [61], the Mn^{2+} ions are in a trigonal bipyramidal environment with one bond to a S atom of the thioantimonate anion. Its isostructural compounds are $\{[M(tren)](Sb_4S_7)\}$ (M = Fe(159), Co(160) and Zn(161)) [61]. Compared with compounds 158–161, the Ni^{2+} ion in $\{[Ni(tren)](Sb_4S_7)\}$(162) [40b] is octahedral coordinated by 4N and 2S atoms, and displays the different binding mode (Fig. 32b). The compounds $[M(teta)][Sb_4S_7]$ (M = Zn(164), Mn(165)) [40b] with the isomer of tren exhibit a more complex 1D $[Sb_4S_7]^{2-}$ anion with the $[M(teta)]^{2+}$ cations being bound at the periphery of the $[Sb_4S_7]^{2-}$ backbone via a M–S bond (Fig. 32c). But the crystal structure of $[\{Mn(tren)\}(As_4Se_7)]$(163) [52] is significantly different from that of 158–162 (Fig. 33). The structure of $[\{Mn(tren)\}(As_2Se_4)]$(145) [52] is closely related to that of $[\{Mn(tren)\}(As_4Se_7)]$ and contains *vierer* infinite $[AsSe_2{}^-]$ chains with coordinated $[Mn(tren)]^{2+}$ fragments (Fig. 34). The examples of the similar $[M(tren)]^{2+}$ complex cations integrated into thioantimonate(III) poly-anions were also observed in the compounds $\{[Mn(tren)](Sb_2S_4)\}$(142) [50], $\{[Co(tren)](Sb_2S_4)\}$(143) [51] and $\{[M(tren)](Sb_2S_4)\}$ (M = Mn(141), Ni(144)) [50,51]. Though these compounds possess general composition $\{[M(tren)](Sb_2S_4)\}$ with an identical Sb:S ratio, the $[Sb_2S_4]^{2-}$ anions exhibit three different types of crystal structures (Figs. 9b, 35 and 36). Compounds 141 and 142 were obtained under identical synthesis conditions but after different reaction time. This observation evidences that

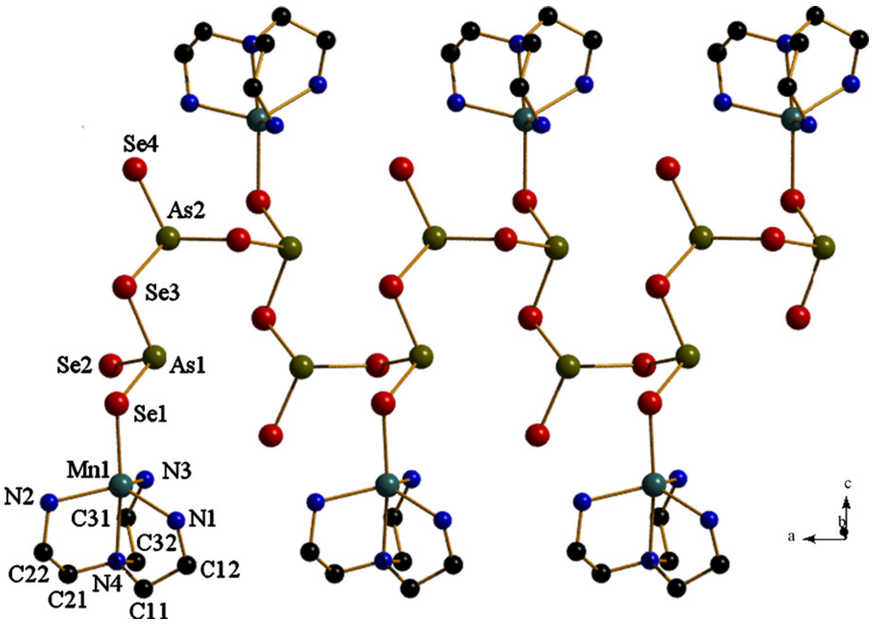

Fig. 34. A segment of the infinite *vierer* chains of $[\{Mn(tren)\}(As_2Se_4)]$(145) [52].

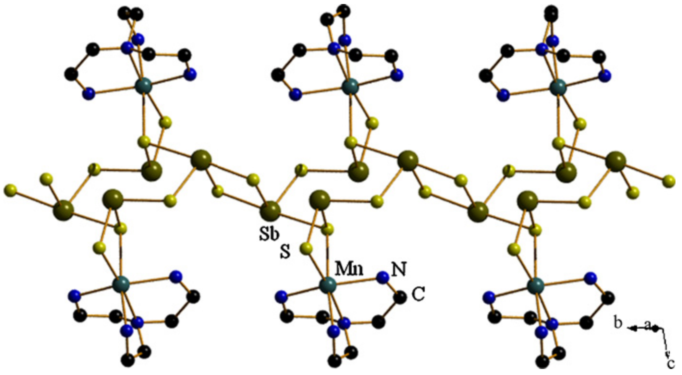

Fig. 35. The crystal structure of $\{[Mn(tren)](Sb_2S_4)\}$(142) [50].

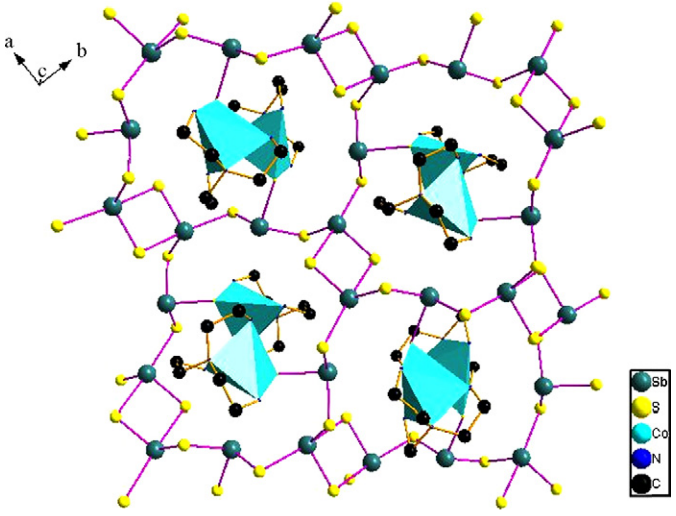

Fig. 36. The crystal structure of $\{[Co(tren)](Sb_2S_4)\}$(143) [51] viewed along [0 0 1]. The [Co(tren)S] trigonal bipyramidal are highlighted by polyhedrons.

the reaction time has a significant effect onto the structures of the thioantimonate(III) anions. Besides two different 1D $[Sb_2S_4]^{2-}$ anionic chains, a 2D $[Sb_2S_4]^{2-}$ anionic network has been found for 143. The cavities of the $Sb_{10}S_{10}$ rings are filled by the $[Co(tren)]^{2+}$ ions (Fig. 36). The Co^{2+} ion is coordinated by four N atoms of the tren ligand, and one S atom of the polymeric $[Sb_2S_4]^{2-}$ anion yielding a trigonal bipyramidal environment.

Some tetrahedral MS_4 species ($M = Mn^{2+}$, Fe^{3+}) share common corners or edges with the SbS_3 pyramids to form a variety of heterobimetallic anions as ligands, including oligonuclear (0D), chainlike (1D) and layered (2D) extended systems. A spectacular example of the thioantimonate(III) with oligonuclear anionic ligand is provided by $\{[Mn(tren)]_4(Mn_2Sb_4S_{12})\}$(167) [62] containing the interesting heterobimetallic $Mn_2Sb_4S_{12}$ core (Fig. 37a). The $[Mn(tren)]^{2+}$ cations are located at the periphery of the core and are bound to the $[Mn_2Sb_4S_{12}]$ unit via two S atoms. Another example for this type analogue is $\{[Mn(tren)]_2(Mn_2Sb_4S_{10})\}$(168) [54] with a new heterobimetallic $[Mn_2Sb_4S_{10}]$core (Fig. 37b). This core may be viewed as a complex tetradentate ligand which is bound to two further $[Mn(tren)]^{2+}$ complex cations. Two interesting examples of the 1D thioantimonates(III) are $\{[Fe(tren)](FeSbS_4)\}$(166) [43] and $[Mn_2(en)(Sb_2S_5)]$(153) [59]. In the former compound, the $[Fe_2S_6]$ bitetrahedron is joined with two SbS_3 units to form the 1D $[FeSbS_4]^{2-}$ chain (Fig. 38). The $[Fe(tren)]^{2+}$ cation is located at the periphery of the chain. In the latter compound, the primary building units are heterocubane-like secondary building unit (SBU) (Fig. 39a). The SBU's are joined via two Mn2–S1 bonds and two long Sb2–S3 contacts and arranged with parallel aligned faces forming chains. Pairs of these chains are linked again through Mn2–S1 bonds of heterocubanes into double-strings (Fig. 39b). It is noteworthy that the structure of 153 exhibits similar building units as all other members of the $[Mn_2(L)(Sb_2S_5)]$ (L = other chelating amine) family [56–58], however with a distinctly different connection scheme. The compounds $[Mn_2(L)(Sb_2S_5)]$ possess a distinct 2D linkage and $[Mn_2(dape)(Sb_2S_5)]$(149) [56] serves as an example and the structural features are discussed here in detail (Fig. 40). The primary building blocks are joined to form $Mn_2Sb_2S_4$ hetero-cubane units which are then connected via common corners, edges and faces into layers with ellip-

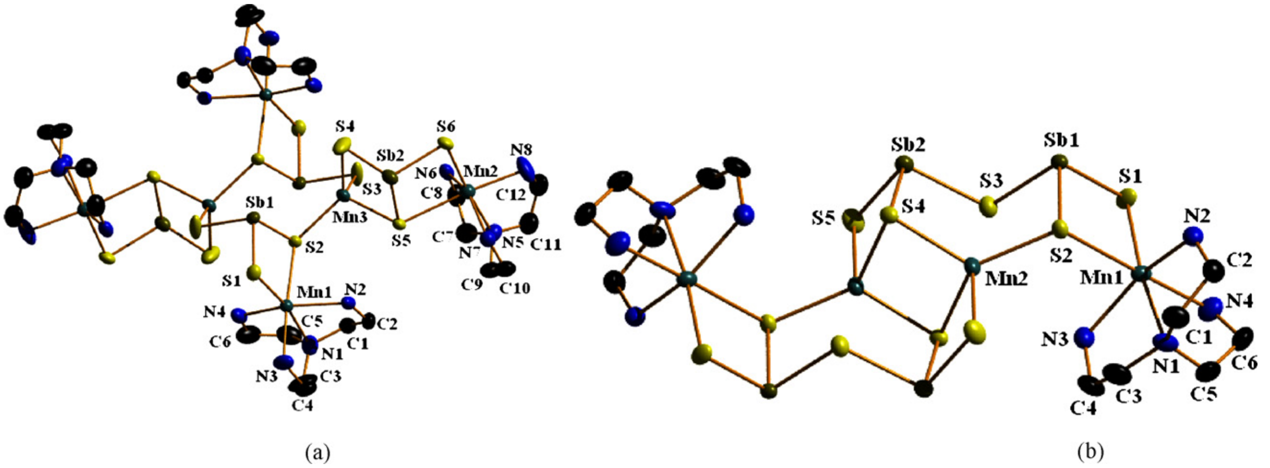

(a) (b)

Fig. 37. Crystal structures of the compounds $\{[Mn(tren)]_4(Mn_2Sb_4S_{12})\}$(167) [62] (a) and $\{[Mn(tren)]_2(Mn_2Sb_4S_{10})\}$(168) [54] (b).

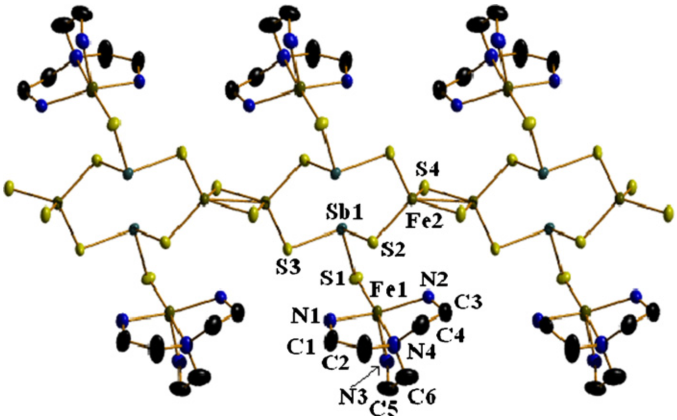

Fig. 38. Crystal structure of $\{[Fe(tren)](FeSbS_4)\}$(166) [43].

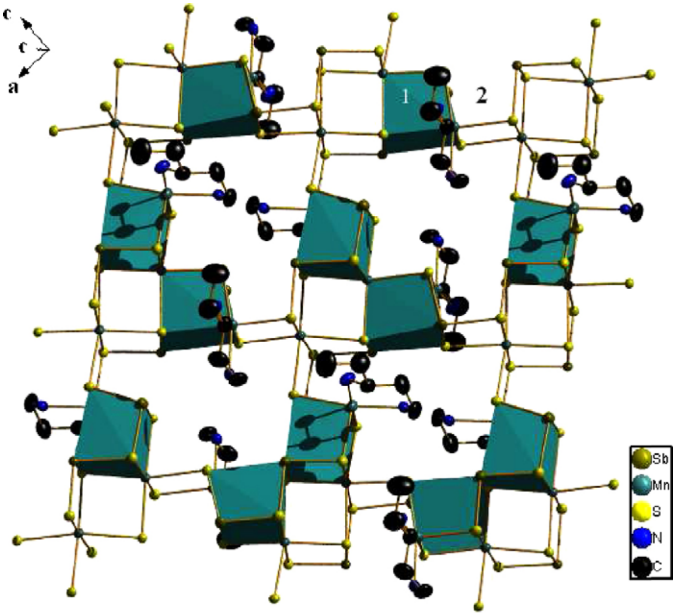

Fig. 40. The layered structure in $[Mn_2(dape)(Sb_2S_5)]$(149) [56] with the two different hetero-cubanes **1** and **2**. The hetero-cubane **1** is highlighted as polyhedra.

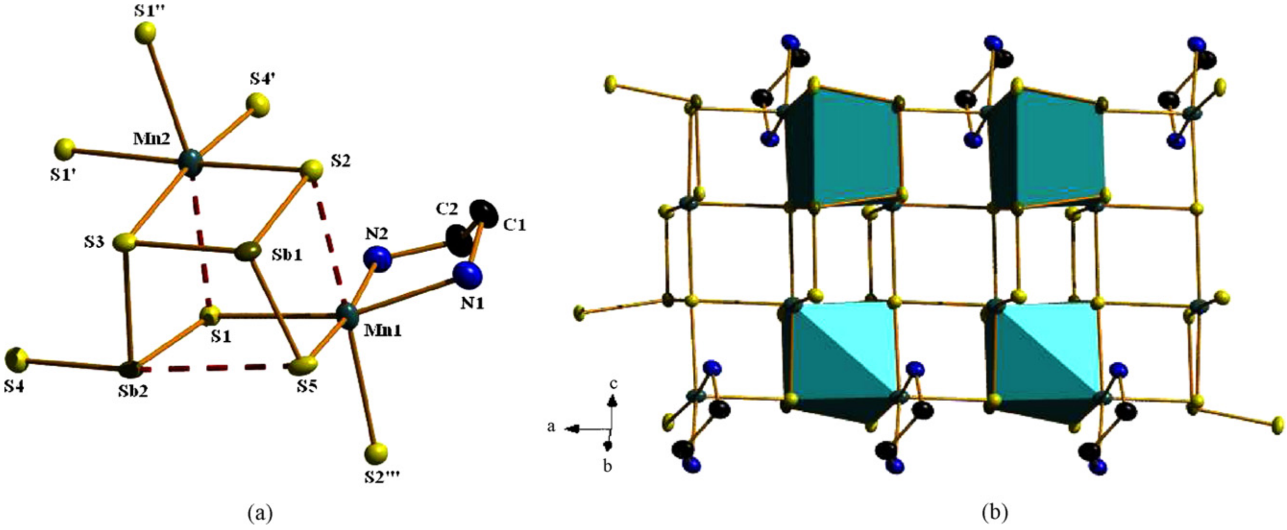

(a) (b)

Fig. 39. (a) The heterocubane-like unit in $[Mn_2(en)(Sb_2S_5)]$(153) [59]. (b) Interconnection of the heterocubane units in 153.

soidal pores in the (0 0 1) plane. The N atoms of dape ligands are exclusively bound to one of the two crystallographically independent Mn^{2+} cations and they point into the pores and between the layers. Similar 2D layered thioantimonates(III) have been obtained by using non-chelating amines as the structure directing agents under solvothermal conditions, such as $[Mn_2(MA)(Sb_2S_5)]$ (MA = methylamine) [59] and $[Mn_2(EA)(Sb_2S_5)]$ (EA = ethylamine) [85]. H-bonding interaction between the amino group and a neighboring sulfur atom not only induces the formation of the 2D structure, but also stabilizes the whole 2D layered structure. As a result, the framework of 153 is obtained with two nearly equally strong hydrogen bonds instead of one. This observation demonstrates that the hydrogen bonding pattern has a significant structure directing effect onto the structure of the thioantimonate(III) anion.

4. Summary

In this review, a survey of the recent developments in solvothermal synthesis of main group chalcogenidometalates applying multidentate/chelating amines is provided. A comprehensive outline of these compounds with metal complex cations has also been presented. The chelating amine is not only an excellent solvent, but at least performs two other important roles: (1) offering a chalcogenide source by reacting with chalcogen elements, a role similar to the non-chelating amines; (2) chelating transition metal or lanthanide metal ions forming large $[M(amine)_x]^{n+}$ counterions to stabilize frameworks of the chalcogen-containing anions and act as unique structure directing or decorating agents. These complex cations can be divided into saturated complex cations and unsaturated complex cations. Usually, tetra- or pentadentate chelating amines, or lanthanide ions have been used to form a complex cation with an unsaturated coordination sphere. The unsaturated complex cations are able to further bond into the primary chalcogenometalate networks, for which a great diversity of structures can be expected. A good relationship between dimensionality of the main group chalcogenidometalate anions and the size of charge balancing counter ion (complex cation) is observed. The chalcogenidometalates exhibit a greater tendency for the formation of low dimensional structures with increasing size of the cation. The effects of the chelating amines on the crystal structures have been systematically presented in the outline from Group 13 to Group 15 chalcogenidometalate anions. Although numerous compounds of this class have been prepared and some of these compounds show interesting optical properties and behave like semiconductors, the exploring and studying on their properties are still insufficient. For this reason, their physical properties have not been summarized in this survey. But much more systematic investigations of the physical properties are needed to establish structure-properties relationships. Without such knowledge, the in situ solvothermal syntheses will have always an explorative and trial-and-error character. Hence, not only a more rigorous characterization of the physical properties of such compounds is a challenge for future research, but also systematic studies are necessary to acquire about the reaction mechanisms occurring under these conditions.

Acknowledgements

This work was supported by the National Natural Science Foundation (Grants 20371033), State Key Laboratory of Coordination Chemistry, Nanjing University, Nanjing, PR China. We also thank Dr. Q.-Y. Zhu and Dr. D.-X. Jia for their valuable contributions to the present work.

References

[1] (a) N.F. Zheng, X.H. Bu, B. Wang, P.Y. Feng, Science 298 (2002) 2366;
(b) J.B. Parise, Science 251 (1991) 293;
(c) H. Li, A. Laine, M. O'Keeffe, O.M. Yaghi, Science 283 (1999) 1145;
(d) T. Jiang, A. Lough, G.A. Ozin, R.L. Bedard, R. Broach, J. Mater. Chem. 8 (1998) 721;
(e) H. Ahari, A. Lough, S. Petrov, G.A. Ozin, R.L. Bedard, J. Mater. Chem. 9 (1999) 1263;
(f) R.L. Bedard, S.T. Wilson, L.D. Vail, J.M. Bennett, E.M. Flanigen, in: P.A. Jacobs, R.A. van Santen (Eds.), Zeolites: Facts, Figures, Future, Proceedings of the 8th International Zeolite Conference, Elsevier, Amsterdam, 1989, p. 375;
(g) O.M. Yaghi, Z. Sun, D.A. Richardson, T.L. Groy, J. Am. Chem. Soc. 116 (1994) 807.

[2] (a) W.S. Sheldrick, M. Wachhold, Angew. Chem. Int. Ed. Engl. 36 (1997) 206;
(b) A. Rabenau, Angew. Chem. Int. Ed. Engl. 24 (1985) 1026;
(c) J. Li, Z. Chen, R.-J. Wang, D.M. Proserpio, Coord. Chem. Rev. 190–192 (1999) 707;
(d) S. Dehnen, M. Melullis, Coord. Chem. Rev. 251 (2007) 1259.

[3] B. Krebs, Angew. Chem. Int. Ed. Engl. 22 (1983) 113.

[4] (a) W.S. Sheldrick, Z. Naturforsch. Teil B 43 (1988) 249;
(b) W.S. Sheldrick, H.G. Braunbeck, Z. Naturforsch. Teil B 47 (1992) 151;
(c) W.S. Sheldrick, B. Schaaf, Z. Naturforsch. Teil B 49 (1995) 655;
(d) H.A. Graf, H. Schäfer, Z. Anorg. Allg. Chem. 414 (1975) 211;
(e) B. Eisenmann, H. Schwerer, H. Schäfer, Mater. Res. Bull. 18 (1983) 383;
(f) C. Brinkmann, B. Eisenmann, H. Schäfer, Mater. Res. Bull. 20 (1985) 299.

[5] W.S. Sheldrick, M. Wachhold, Coord. Chem. Rev. 176 (1998) 211.

[6] (a) A. Fehlker, R. Blachnik, Z. Anorg. Allg. Chem. 627 (2001) 411;
(b) V. Spetzler, C. Näther, W. Bensch, Inorg. Chem. 44 (2005) 5805;
(c) A.V. Powell, S. Boissière, Chem. Mater. 12 (2000) 182;
(d) Y.J. Dong, Q. Peng, R.J. Wang, Y.D. Li, Inorg. Chem. 42 (2003) 1794;
(e) C.L. Cahill, B. Gugliotta, J.B. Parise, Chem. Commun. (1998) 1715;
(f) D. Pitzschke, C. Näther, W. Bensch, Solid State Sci. 4 (2002) 1167.

[7] (a) X.H. Bu, N.F. Zheng, X.Q. Wang, B. Wang, P.Y. Feng, Angew. Chem. Int. Ed. 43 (2004) 1502;
(b) H.L. Li, J. Kim, M. O'Keeffe, O.M. Yaghi, Angew. Chem. Int. Ed. 42 (2003) 1819;
(c) H.L. Li, M. Eddaoudi, A. Laine, M. O'Keeffe, O.M. Yaghi, J. Am. Chem. Soc. 121 (1999) 6096;
(d) X.H. Bu, N.F. Zheng, Y.Q. Li, P.Y. Feng, J. Am. Chem. Soc. 125 (2003) 6024.

[8] P.Y. Feng, X.H. Bu, N.F. Zheng, Acc. Chem. Res. 38 (2005) 293.

[9] H. Stephan, M.G. Kanatzidis, J. Am. Chem. Soc. 118 (1996) 12226.

[10] (a) R. Kiebach, F. Studt, C. Näther, W. Bensch, Eur. J. Inorg. Chem. (2004) 2553;
(b) M. Schur, H. Rijnberk, C. Näther, W. Bensch, Polyhedron 18 (1999) 101;
(c) W. Bensch, C. Näther, R. Stahler, Chem. Commun. (2001) 477;
(d) P. Vaqueiro, A.M. Chippindale, A.V. Powell, Inorg. Chem. 43 (2004) 7963;
(e) M.R. Girard, J. Li, D.M. Proserpio, Main Group Met. Chem. 21 (1998) 231.

[11] (a) P. Vaqueiro, Inorg. Chem. 45 (2006) 4150;
(b) M. Behrens, S. Scherb, C. Näther, W. Bensch, Z. Anorg. Allg. Chem. 629 (2003) 1367.

[12] Q.C. Zhang, X.H. Bu, Z.E. Lin, M. Biasini, W.P. Beyermann, P.Y. Feng, Inorg. Chem. 46 (2007) 7262.

[13] (a) J. Zhou, G.-Q. Bian, Y. Zhang, Q.-Y. Zhu, C.-Y. Li, J. Dai, Inorg. Chem. 46 (2007) 6347;
(b) J. Zhou, Y. Zhang, G.-Q. Bian, Q.-Y. Zhu, C.-Y. Li, J. Dai, Cryst. Growth Des. 9 (2007) 1889;
(c) J. Zhou, Y. Zhang, G.-Q. Bian, C.-Y. Li, X.-X. Chen, J. Dai, Cryst. Growth Des. 8 (2008) 2235;
(d) J. Zhou, Y. Zhang, A.-B. Tang, G.-Q. Bian, D.-X. Jia, J. Dai, Inorg. Chem. Commun. 10 (2007) 348;
(e) J. Zhou, G.-Q. Bian, J. Dai, Y. Zhang, A.-B. Tang, Q.-Y. Zhu, Inorg. Chem. 46 (2007) 1541;
(f) D.-X. Jia, Y. Zhang, J. Dai, Q.-Y. Zhu, X.-M. Gu, Z. Anorg. Allg. Chem. 630 (2004) 313;
(g) D.-X. Jia, J. Dai, Q.-Y. Zhu, Y. Zhang, X.-M. Gu, Polyhedron 23 (2004) 937;
(h) D.-X. Jia, J. Dai, Q.-Y. Zhu, L.-H. Cao, H.-H. Lin, J. Solid State Chem. 178 (2005) 874;
(i) X.-M. Gu, J. Dai, D.-X. Jia, Y. Zhang, Q.-Y. Zhu, Cryst. Growth Des. 5 (2005) 1845;
(j) D.-X. Jia, Y. Zhang, J. Dai, Q.-Y. Zhu, X.-M. Gu, J. Solid State Chem. 177 (2004) 2477;
(k) D.-X. Jia, Q.-X. Zhao, J. Dai, Y. Zhang, Q.-Y. Zhu, Z. Anorg. Allg. Chem. 632 (2006) 349;
(l) J. Zhou, G.-Q. Bian, Y. Zhang, J. Dai, N. Cheng, Z. Anorg. Allg. Chem. 633 (2007) 2701;
(m) D.X. Jia, A. Zhu, Y. Zhang, J. Deng, Monatsh. Chem. 138 (2007) 191;
(n) J. Zhou, C.-Y. Li, Y. Zhang, J. Dai, J. Coord. Chem, in press;
(o) G.Q. Bian, J. Zhou, C.Y. Li, N. Cheng, X.M. Lin, Y. Zhang, J. Dai, Chem. Res. Appl. 20 (2008) 53.

[14] (a) D.-X. Jia, A.-M. Zhu, J. Deng, Y. Zhang, Z. Anorg. Allg. Chem. 633 (2007) 1246;
(b) Q.X. Zhao, D.X. Jia, Y. Zhang, L.F. Song, J. Dai, Inorg. Chim. Acta 360 (2007) 1895;
(c) D.X. Jia, Q.X. Zhao, Y. Zhang, J. Dai, J.L. Zuo, Inorg. Chem. 44 (2005) 8861;
(d) D.-X. Jia, Q.-Y. Zhu, J. Dai, W. Lu, W.-J. Guo, Inorg. Chem. 44 (2005) 819;
(e) D.-X. Jia, J. Deng, Q.-X. Zhao, Y. Zhang, J. Mol. Struct. 833 (2006) 114;
(f) D.-X. Jia, Q.-X. Zhao, Y. Zhang, J. Dai, J. Zhou, Eur. J. Inorg. Chem. (2006) 2760;

(g) C.-Y. Li, J. Zhou, Y. Zhang, J. Dai, Inorg. Chem. Commun, in press.;
(h) C.-Y. Li, J. Zhou, Y. Zhang, G.-Q. Bian, J. Dai, Acta Crystallogr., in press;
(i) D.X. Jia, A.M. Zhu, J. Deng, Y. Zhang, J. Dai, Dalton Trans. (2007) 2083.
[15] Z. Chen, J. Li, F. Chen, D.M. Proserpio, Inorg. Chim. Acta 273 (1998) 255.
[16] J. Li, Z. Chen, T.J. Emge, D.M. Proserpio, Inorg. Chim. 36 (1997) 1437.
[17] X.A. Chen, X.Y. Huang, J. Li, Inorg. Chem. 40 (2001) 1341.
[18] M.-L. Fu, G.-C. Guo, B. Liu, A.-Q. Wu, J.-S. Huang, Chin. J. Inorg. Chem. 21 (2005) 25.
[19] H.-B. Duan, Z. Hu, B. Jia, Y.-L. An, Acta Crystallogr. E62 (2006) m2709.
[20] Z. Chen, R.J. Wang, Acta Phys. Chim. Sin. 15 (1999) 1070.
[21] J. Li, Z. Chen, T.J. Emge, T. Yuen, D.M. Proserpio, Inorg. Chim. Acta 273 (1998) 310.
[22] E. Ruzin, C. Zimmermann, P. Hillebrecht, S. Dehnen, Z. Anorg. Allg. Chem. 633 (2007) 820.
[23] J.L. Shreeve-Keyer, C.J. Warren, S.S. Dhingrat, R.C. Haushalter, Polyhedron 16 (1997) 1193.
[24] Z. Chen, R.-J. Wang, J. Li, Chem. Mater. 12 (2000) 762.
[25] T.V. Almsick, A. Loose, W.S. Sheldrick, Z. Anorg. Allg. Chem. 631 (2005) 21.
[26] N.F. Zheng, X.H. Bu, P.Y. Feng, Chem. Commun. (2005) 2805.
[27] (a) A. Kromm, W.S. Sheldrick, Acta Crystallogr. E62 (2000) m2767;
(b) A. Kromm, W.S. Sheldrick, Z. Anorg. Allg. Chem. 634 (2008) 1005.
[28] M. Melullis, M.K. Brandmayer, S. Dehnen, Z. Anorg. Allg. Chem. 632 (2006) 64.
[29] M. Schur, W. Bensch, Acta Crystallogr. 56C (2000) 1107.
[30] R. Stahler, C. Näther, W. Bensch, Acta Crystallogr. 57C (2001) 26.
[31] (a) Q.-X. Zhao, J. Deng, D.-X. Jia, Y. Zhang, J. Dai, Chem. Res. Appl. 18 (2006) 823;
(c) M.-L. Fu, W.-T. Chen, L.-Z. Cai, B. Liu, G.-C. Guo, J.-S. Huang, Chin. J. Struct. Chem. 23 (2004) 731;
(d) F. Wendland, C. Näther, M. Schur, W. Bensch, Acta Crystallogr. 54C (1998) 317.
[32] R.J.E. Lees, A.V. Powell, A.M. Chippindale, Polyhedron 24 (2005) 1941.
[33] D.X. Jia, Y. Zhang, Q.X. Zhao, J. Deng, Inorg. Chem. 45 (2006) 9812.
[34] Z. Chen, R.-J. Wang, X.-Y. Huang, J. Li, Acta Crystallogr. C56 (2000) 1100.
[35] D.-X. Jia, Q.-X. Zhao, L.-F. Song, Y. Zhang, J. Dai, Chin. J. Struct. Chem. 25 (2006) 1110.
[36] M.-L. Fu, G.-C. Guo, X. Liu, B. Liu, L.-Z. Cai, J.-S. Huang, Inorg. Chem. Commun. 8 (2005) 18.
[37] H. Stephan, M.G. Kanatzidis, Inorg. Chem. 36 (1997) 6050.
[38] P. Vaqueiroa, D.P. Darlowa, A.V. Powella, A.M. Chippindale, Solid State Ionics 172 (2004) 601.
[39] W. Bensch, M. Schur, Z. Naturforsch. 27b (1996) 405.
[40] (a) R. Stähler, C. Näther, W. Bensch, J. Solid State Chem. 174 (2003) 264;
(b) H. Lühmann, Z. Rejai, K. Möller, P. Leisner, M. Ordolff, C. Näther, W. Bensch, Z. Anorg. Allg. Chem. 634 (2008) 1687.
[41] A.V. Powell, R.J.E. Lees, A.M. Chippindale, Inorg. Chem. 45 (2006) 4261.
[42] R. Stähler, B. Mosel, H. Eckert, W. Bensch, Angew. Chem. Int. Ed. 41 (2002) 4487.
[43] R. Kiebach, W. Bensch, R. Hoffmann, R. Pöttgen, Z. Anorg. Allg. Chem. 629 (2003) 532.
[44] R. Stähler, C. Näther, W. Bensch, Eur. J. Inorg. Chem. (2001) 1835.
[45] R. Stähler, W. Bensch, Z. Anorg. Allg. Chem. 628 (2002) 1657.
[46] P. Vaqueiro, A.M. Chippindale, A.V. Powell, Polyhedron 22 (2003) 2839.
[47] M. Schaefer, L. Engelke, W. Bensch, Z. Anorg. Allg. Chem. 629 (2003) 1912.
[48] T.V. Almsick, W.S. Sheldrick, Z. Anorg. Allg. Chem. 632 (2006) 1413.
[49] W. Bensch, C. Näther, M. Schur, Chem. Commun. (1997) 1773.
[50] M. Schaefer, D. Kurowski, A. Pfitzner, C. Näther, Z. Rejai, K. Möller, N. Ziegler, W. Bensch, Inorg. Chem. 45 (2006) 3726.
[51] R. Stähler, W. Bensch, Eur. J. Inorg. Chem. (2001) 3073.
[52] A. Kromm, W.S. Sheldrick, Z. Anorg. Allg. Chem. 634 (2008) 225.
[53] A. Kromm, W.S. Sheldrick, Z. Anorg. Allg. Chem. 634 (2008) 121.
[54] M. Schaefer, C. Näther, N. Lehnert, W. Bensch, Inorg. Chem. 43 (2004) 2914.
[55] R. Stahler, W. Bensch, J. Chem. Soc., Dalton Trans. (2001) 2518.
[56] A. Puls, C. Näther, W. Bensch, Z. Anorg. Allg. Chem. 632 (2006) 1239.
[57] W. Bensch, M. Schur, Eur. J. Solid State Inorg. Chem. 33 (1996) 1149.
[58] L. Engelke, R. Stahler, M. Schur, C. Näther, W. Bensch, R. Pottgen, M.H. Moller, Z. Naturforsch. B: Chem. Sci. 59 (2004) 869.
[59] M. Schur, W. Bensch, Z. Naturforsch. B: Chem. Sci. 57 (2002) 1.
[60] M. Schaefer, C. Näther, W. Bensch, Monatsh.Chem. 135 (2004) 461.
[61] M. Schaefer, R. Stähler, W. Kiebach, C. Näther, W. Bensch, Z. Anorg. Allg. Chem. 630 (2004) 1816.
[62] M. Schaefer, C. Näther, W. Bensch, Solid State Sci. 5 (2003) 1135.
[63] (a) M.-L. Fu, G.-C. Guo, L.-Z. Cai, Z.-J. Zhang, J.-S. Huang, Inorg. Chem. 44 (2005) 184;
(b) M.-L. Fu, G.-C. Guo, X. Liu, W.-T. Chen, B. Liu, J.-S. Huang, Inorg. Chem. 45 (2006) 5793.
[64] (a) P.J. Hagrman, D. Hagrman, J. Zubieta, Angew. Chem. Int. Ed. 38 (1999) 2638;
(b) J.-K. Cheng, Y.-G. Yao, J. Zhang, Z.-J. Li, Z.-W. Cai, X.-Y. Zhang, Z.-N. Chen, Y.-B. Chen, Y. Kang, Y.-Y. Qin, Y.-H. Wen, J. Am. Chem. Soc. 126 (2004) 7796;
(c) D. Hagrman, P.J. Hagrman, J. Zubieta, Angew. Chem. Int. Ed. 38 (1999) 3165.
[65] (a) C.-S. Liu, X.-S. Shi, J.-R. Li, J.-J. Wang, X.-H. Bu, Cryst. Growth Des. 6 (2006) 656;
(b) P.-K. Chen, Y.-X. Che, L. Xue, J.-M. Zheng, Cryst. Growth Des. 6 (2006) 2517;
(c) T. Ohmura, A. Usuki, K. Fukumori, T. Ohta, M. Ito, K. Tatsumi, Inorg. Chem. 45 (2006) 7988.
[66] Y.L. An, B. Menghe, L. Ye, M. Ji, X. Liu, G.L. Ning, Inorg. Chem. Commun. 8 (2005) 301.
[67] S.S. Dhingra, R.C. Haushalter, Chem. Mater. 6 (1994) 2376.
[68] E.R. Franke, H. Schäfer, Z. Naturforsch. B 37 (1972) 1308.
[69] Y.-C. Hung, S.-J. Hwu, Acta Crystallogr. C49 (1993) 1588.
[70] D. Miiller, G. Eulenberger, H. Hahn, Z. Anorg. Allg. Chem. 398 (1973) 207.
[71] W. Klee, H. Schäfer, Z. Anorg, Allg. Chem. 479 (1981) 125.
[72] P. Vaqueiro, J. Solid State Chem. 179 (2006) 302.
[73] C.J. Warren, S.S. Dhingra, R.C. Haushalter, A.B. Bocarsly, J. Solid State Chem. 112 (1994) 340.
[74] C. Wang, R.C. Haushalter, Inorg. Chem. 36 (1997) 3806.
[75] W.S. Sheldrick, J. Kaub, Z. Naturforsch. Teil B 40 (1985) 19.
[76] W.S. Sheldrick, J. Kaub, Z. Naturforsch. Teil B 40 (1985) 1020.
[77] T. König, B. Eisenmann, H. Schäfer, Z. Anorg. Allg. Chem. 488 (1982) 126.
[78] W.S. Sheldrick, H.-J. Häusler, Z. Anorg. Allg. Chem. 561 (1988) 139.
[79] V. Vater, W.S. Sheldrick, Z. Naturforsch. Teil B 52 (1997) 1119.
[80] J.B. Parise, Y. Ko, Chem. Mater. 4 (1992) 1446.
[81] G. Dittmar, H. Schäfer, Z. Anorg. Allg. Chem. 437 (1977) 183.
[82] Q.C. Zhang, X.H. Bu, L. Han, P.Y. Feng, Inorg. Chem. 45 (2006) 6684.
[83] M. Behrens, C. Näther, W. Bensch, Z. Anorg. Allg. Chem. 628 (2002) 2160.
[84] (a) H. Sommer, R. Hoppe, Z. Anorg. Allg. Chem. 430 (1997) 199;
(b) H.Y.P. Hong, J.C. Mikkelsen Jr., G.W. Roland, Mater. Res. Bull. 9 (1974) 365;
(c) A. Olsen, P. Goodman, H.J. Whitfield, J. Solid State Chem. 60 (1985) 305.
[85] M. Schur, C. Näther, W. Bensch, Z. Naturforsch. B: Chem. Sci. 56 (2001) 79.